THESIS

THE AUTISM-ASSOCIATED LOSS OF δ-CATENIN FUNCTION DISRUPTS SOCIAL BEHAVIOR

Submitted by

Hadassah Mendez-Vazquez

Department of Biomedical Sciences

In partial fulfillment of the requirements

For the Degree of Master of Science

Colorado State University

Fort Collins, Colorado

Summer 2023

Master's Committee:

Advisor: Seonil Kim

Soham Chanda
Brent Myers
Michael Tamkun

ABSTRACT

THE AUTISM-ASSOCIATED LOSS OF δ-CATENIN FUNCTION DISRUPTS SOCIAL BEHAVIOR

Social impairment is a key symptom of several neuropsychiatric disorders, including autism spectrum disorder (ASD), anxiety, depression, and schizophrenia. Despite the increasing prevalence of these disorders the physiological, cellular, and molecular factors underlying social dysfunction are still poorly understood. In humans, mutations in the *δ-catenin* gene have been linked to severe forms of ASD. δ-catenin is a post-synaptic scaffolding protein that is expressed in excitatory synapses and functions as an anchor for N-cadherin and the AMPA receptor (AMPAR) subunit GluA2 at the postsynaptic density. A glycine 34 to serine (G34S) mutation in the *δ-catenin* gene was identified in ASD patients and induces a loss of δ-catenin function, which may mediate ASD pathogenesis. The mechanism by which this G34S mutation causes loss of δ-catenin function to induce ASD remains unclear. Initial findings revealed that the G34S mutation increases glycogen synthase kinase 3β (GSK3β)-dependent δ-catenin degradation to reduce δ-catenin levels. Moreover, we found that mice possessing the G34S δ-catenin mutation have significantly reduced synaptic cortical δ-catenin and GluA2 levels. The G34S mutation was also found to differentially alter glutamatergic activity in cortical excitatory and inhibitory cells. Furthermore, G34S δ-catenin mutant mice exhibit markedly impaired social behavior, which is a characteristic feature of ASD. Most significantly, we found that inhibition of GSK3β is sufficient to reverse the G34S-induced loss of δ-catenin function in cells and mice. Altogether, our study reveals that the loss of δ-catenin function arising from the ASD-associated G34S mutation induces social dysfunction via disruptions in glutamatergic activity, and that GSK3β inhibition can reverse abnormal δ-catenin G34S-induced glutamatergic activity and social deficits.

ACKNOWLEDGEMENTS

I would like to thank each of those who contributed to this work, especially Kaila Nip and Matheus Sathler, who generated all the foundational data upon which this whole study is built. I would like to acknowledge the hard work of all the students who have taken part many aspects of this very large project. Without the teamwork of the students of the Kim lab, this work would not have been possible. I am also extremely grateful to my committee members, Dr. Michael Tamkun, Dr. Brent Myers and Dr. Soham Chanda, for their excellent support and valuable critiques which have resulted in the profound betterment of this work.

I would like to thank my husband, Ricardo for his persistent love and unending support throughout this journey. Were it not for his encouragement, companionship and sensible outlook on life, I never would have made it through this degree. He is truly my rock, and I am constantly thankful that he has been by my side throughout this journey. I would also like to thank Rahmi Lee for being my lab therapist, my confidant for every failed experiment, and a true friend. I will never be able to thank her enough for believing in me more than I believe in myself.

I would like to thank every mentor I have had in my time at Colorado State University, especially Dr. Michael Tamkun and Dr. Shane Kanatous. In their own way, they both have taught me to toughen up, own my work, and never shy away from moving forward.

Finally, I would like to thank Dr. Seonil Kim for being the best mentor I know and a more long-suffering advisor than I have ever deserved. None of this work would have been possible without his excellent direction, boundless dedication to his students, and his tireless enthusiasm for science. His patient support and instruction over the last four years has allowed me to grow from a lost kid with a cluttered head and love for science into a high functioning sociopath with a science addiction. It is one of the greatest honors of my life to have been one of his “kids” and to be a part of his continuing “DNA”.

TABLE OF CONTENTS

LIST OF TABLES

LIST OF FIGURES

INTRODUCTION[1]

The ability to engage in social behavior is essential for the existence of many species. While much work has been done to investigate the mechanisms that underlie this complex behavior, much remains to be understood (1). Social dysfunction is a significant component of a variety of neuropsychiatric disorders, including anxiety, depression, and neurodevelopmental disorders like autism spectrum disorder (ASD) (2). The study of pathologies like ASD, that contain a significant social deficit component, allow for deeper inspection of the processes that underlie social behavior itself.

Autism spectrum disorder is a neurodevelopmental disorder characterized by social behavior dysfunction as well as restricted and repetitive behaviors. Studies investigating the origin and onset of ASD have increased in prevalence the last decade, thereby increasing our collective understand of the genetic components of the disorder. Of these studies, a significant number have identified abnormal synaptic function as a core component contributing to the onset of ASD. Moreover, excitatory connectivity is strong implicated in patients with ASD and in mouse models of the disorder (3-11). Still, the mechanisms by which glutamatergic activity mediates the behavioral abnormalities associated with ASD, particularly social dysfunction, are unknown. A growing body of studies illustrate that altered synaptic activity and signaling could contribute to the neural activity underlying social behavior (1). The postsynaptic glutamatergic activity in excitatory and inhibitory cells in several brain areas has been identified as important for social behavior (6-10). However, the role synaptic regulation plays in maintaining proper social behavior is not well understood.

Although many proteins related to synaptic structure and function have been implicated

[1] Published as: Mendez-Vazquez, Hadassah, et al. “The Autism-Associated Loss of δ-Catenin Functions Disrupts Social Behaviors.” Proceedings of the National Academy of Sciences, 2023, https://doi.org/10.1101/2023.01.12.523372.

as strong ASD-risk genes, recent studies suggest that the gene for the synaptic scaffolding protein δ-catenin is strongly linked to ASD (12-16). Genetic alterations in the *δ-catenin* gene have been recently discovered in ASD individuals from multiple families (13, 15, 16). δ-catenin is characterized as a member of the armadillo repeat protein family and is primarily expressed in neurons where it is localized to the post synaptic density (PSD) of excitatory and inhibitory synapses (25-31). In the excitatory PSD, δ-catenin interacts with the intracellular domain of N-cadherin, a synaptic adhesion protein, and the carboxyl terminus portion of δ-catenin binds the glutamate receptor-interacting protein (GRIP) and AMPA-type glutamate receptor (AMPAR)-binding protein (ABP) complex (Fig. 1) (17-22). The N-cadherin-δ-catenin-GRIP/ABP complex serves as an anchor for the localization of GluA2 AMPA receptor subunits to the post-synaptic membrane. This complex and its anchor function are disrupted when δ-catenin function is lost (17-22).

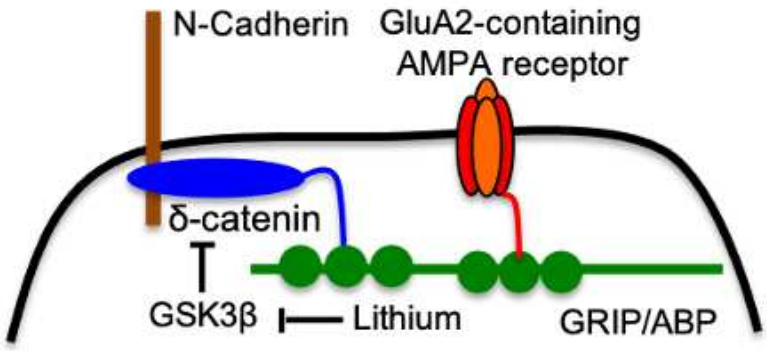

Figure 1. A schematic of N-cadherin-δ-catenin-ABP/GRIP-GluA2 synaptic complex.
A schematic of N-cadherin-δ-catenin-ABP/GRIP-GluA2 synaptic complex and GSK3β regulation of δ-catenin. At the PSD, δ-catenin interacts with N-cadherin, a synaptic cell adhesion protein. The carboxyl-terminus of δ-catenin binds to AMPA receptor-binding protein (ABP) and glutamate receptor-interacting protein (GRIP). This N-cadherin-δ-catenin-ABP/GRIP complex functions as an anchor for GluA2. GSK3β phosphorylates δ-catenin, which leads to δ-catenin degradation. The reduction of GSK3β activity by lithium stabilizes the N-cadherin-δ-catenin-ABP/GRIP-GluA2 complex.

Some δ-catenin ASD-related mutations result in a δ-catenin-deficiency induced loss of excitatory synapses in cultured mouse neurons, suggesting that these mutations cause a loss of δ-catenin function (16).Thus, δ-catenin loss could cause impairment of glutamatergic synapses which may induce ASD-associated social dysfunction. Other autism-risk genes like GRIP,

GluA2, cadherins, and Ras GTPase activating protein 1 (SYNGAP1), which are also involved in synaptic structure and function, are strongly linked to δ-catenin function. This further demonstrates the importance of δ-catenin in synaptic pathophysiology and social dysfunction in ASD (23-26). Still, the molecular and cellular mechanisms linking δ-catenin function, synaptic activity and social behavior are generally unknown. Although there are several known ASD-associated δ-catenin mutations, the glycine 34 to serine (G34S) missense mutation results in a profound loss of δ-catenin function at excitatory synapses (16). However, how the G34S mutation induces such a significant loss of function is largely unknown, especially regarding social dysfunction in ASD.

In this study, we discovered that the G34S δ-catenin mutation results in increased phosphorylation of δ-catenin by glycogen synthase kinase 3β (GSK3β), thereby upregulating δ-catenin degradation. Using δ-catenin G34S knock-in mice, we found that the G34S δ-catenin mutation causes altered glutamatergic synaptic activity in the cortex and impairs social behavior. Additionally, we demonstrate how inhibition of GSK3β activity can reverse the G34S-induced loss of δ-catenin function and recover normal glutamatergic activity and social behavior. Finally, we used a δ-catenin knockout (KO) mouse model to confirm the necessity of δ-catenin for the recovery of normal social behavior in G34S δ-catenin mice due to GSK3β inhibition. Significantly, recent studies indicate that GSK3β activity may be an important component in the pathophysiology of ASD (27-34). GSK3β has long been identified as potentially useful therapeutic target for neuropsychiatric disorders due to the role of GSK3β in cognitive processes (35). Thus, this study both identifies the cellular and molecular mechanisms by which δ-catenin mediates in social behavior, and estalishes GSK3β as a therapeutic target for limiting the effect of δ-catenin deficiency-induced synaptic dysfunction in ASD and related mental disorders.

METHODS AND MATERIALS

Human neuroblastoma cell (SH-SY5Y) culture and transfection

SH-SY5Y cells were grown in DMEM medium with fetal bovine serum (Life Technologies) and 1% penicillin/streptomycin (Life Technologies). 500,000 cells were plated in 6-well dishes and 1 µg of DNA was transfected when cells reached 75-85% confluency with Lipofectamine 2000 (Life Technologies) according to the manufacturer's instructions. 25 nM control siRNA ON-TARGETplus non-targeting pool (Dharmacon siRNA solution) and 25 nM SMARTpool ON-TARGETplus human GSK3β siRNA (Dharmacon siRNA solution) were transfected with 1 µg of DNA when cells reached 50% confluency and cell lysates were collected 72 hours later. Cells used for each experiment were from more than three independently prepared cultures.

DNA Cloning

pSinRep5-WT δ-catenin and pSinRep5-G34S δ-catenin plasmids were gifts from Dr. Edward Ziff (New York University Langone Health). HA-tagged WT δ-catenin and G34S δ-catenin were cloned into the mammalian expression vector, pcDNA3.1. The QuikChange XL Site-Directed Mutagenesis Kit (Agilent Technologies) was used to generate G34A and G34D mutations from the WT δ-catenin plasmid. The following primers were used with the bolded regions being where the mutations were made to exchange the glycine (GGC): G34A primers 5'-GCTCCTTGAGCCCA***GCC***TTAAACACCTCCAA-3' and 5'-TTGGAGGTGTTTAAGGCTGGGCTCAAGGAGC-3', and the G34D primers 5'-CAGCTCCTTGAGCCCA***GAC***TTAAACACCTCCAATG-3' and 5'-CATTGGAGGTGTTTAAGTCTGGGCTCAAGGAGCTG-3'.

Animals

All mice were bred in the animal facility at Colorado State University (CSU). Animals were housed under 12:12 hour light/dark cycle. 3-month-old male and female mice were used in the current study. CSU's Institutional Animal Care and Use Committee (IACUC) reviewed and approved the animal care and protocol (3408). Lithium treatment in animals was conducted as described previously (21). Lithium animals received standard chow containing 0.17% w/w lithium carbonate (Harlan Teklad, Madison, WI) *ad libitum* for 7 days. Control animals were fed with standard chow.

Generation of δ-catenin G34S mice

δ-catenin G34S mice (RRID:MMRRC_050621-UCD) were generated by Dr. Jyothi Arikkath at UNMC Mouse Genome Engineering Core using the CRISPR-Cas9 technique (36)

Primary cortical neuron culture

Postnatal day 0 (P0) male and female pups from WT or G34S δ-catenin mice were used to produce mouse cortical neuron cultures as shown previously (37, 38). Heterozygous G34S mice were used to breed for generating each genotype. PCR was performed to identify each genotype before preparing cultures.

Immunoblotting

Immunoblotting was performed as described previously (21, 37-51). Whole brains were rapidly removed and placed in ice-cold solution A (0.32 M sucrose, 1 mM $NaHCO_3$, 1 mM $MgCl_2$, and 0.5 mM $CaCl_2$) and protease inhibitors. The brains were subjected to dounce homogenization in 40 ml of solution A per 10 g of wet brain tissue. The homogenates were diluted to 10% weight/volume with solution A and centrifuged at 1,400 *g* for 10 min. The

supernatant solution was saved as whole tissue lysates, and the pellet. Supernatants were then spun at 30,000 × *g* for 15 min to obtain a crude P2 fraction. The pellet was resuspended in solution B (0.32 M sucrose and 1 mM $NaHCO_3$) using 24 ml of solution B per 10 g of starting material. This homogenate was layered on top of a 1 M sucrose and 1.2 M sucrose gradients and centrifuged at 82,500 *g* for 2 hr. Purified synaptosomes were collected at the 1 M and 1.2 M sucrose interface and were then collected by centrifugation at 48,200 *g* for 45 min. The pellets were resuspended in 25mM This pH 8.4, and an equal volume of 1% Triton X-100 was added and rocked at 4°C for 30 min. These lysed synaptosomes were centrifuged at 32,800 *g* for 30 min. The PSD pellet was resuspended in 25mM This pH 8.4 with 2% SDS. Equal amounts of protein (whole cell lysates and PSD) were loaded on 10% SDS-PAGE gel and transferred to nitrocellulose membranes. Membranes were blotted with antibodies. The primary antibodies consisted of anti-δ-catenin (BD Biosciences, 1:1000 and Abcam, 1:1000), anti-GluA1 (Millipore, 1:2000), anti-GluA2 (Abcam, 1:2000), anti-pGSK3β (Cell Signaling Technology, 1:1000), and anti-actin (Abcam, 1:2000) antibodies. Protein bands were quantified using ImageJ (https://imagej.nih.gov/ij/).

GCaMP Ca^{2+} Imaging with glutamate uncaging

We carried out Ca^{2+} imaging with glutamate uncaging in cultured mouse cortical neurons to determine glutamatergic activity as described previously (52). For Ca^{2+} imaging, a genetically encoded Ca^{2+} indicator, GCaMP, was used. When AAVs of the same serotype are co-infected, many neurons are transduced by both viruses (53). We thus co-infected AAVs expressing CamK2a-Cre (Addgene #105558-AAV1), pENN.AAV.CamKII 0.4.Cre.SV40 was a gift from James M. Wilson (Addgene plasmid #105558 ; http://n2t.net/addgene:105558 ; RRID:Addgene_105558), and Cre-dependent GCaMP7s (Addgene #104495-AAV1) (54), pGP-AAV-CAG-FLEX-jGCaMP7s-WPRE was a gift from Douglas Kim & GENIE Project

(Addgene plasmid # 104495 ; http://n2t.net/addgene:104495 ; RRID:Addgene_104495), in 4 days *in vitro* (DIV) neurons and imaged 12-13 DIV excitatory neurons. In addition, AAV expressing GCaMP6f under the control of the GABAergic neuron-specific enhancer of the mouse *Dlx* (mDlx) gene (Addgene# 83899-AAV1) (55), pAAV-mDlx-GCaMP6f-Fishell-2 was a gift from Gordon Fishell (Addgene plasmid #83899-AAV1 ; http://n2t.net/addgene:83899 ; RRID:Addgene_83899), was infected in 4 DIV neurons and imaged 12-13 DIV inhibitory interneurons. Glass-bottom dishes were mounted on a temperature-controlled stage on an Olympus IX73 microscope and maintained at 37°C and 5% CO_2 using a Tokai-Hit heating stage and digital temperature and humidity controller. For glutamate uncaging, 1 mM 4-methoxy-7-nitroindolinyl (MNI)-caged L-glutamate was added to the culture media, and epi-illumination photolysis (390 nm, 0.12 mW/mm^2, 1 ms) was used to uncage glutamate in the whole field of view. 2 μM TTX was added to prevent action potential-dependent network activity. A baseline average of 20 frames (10 ms exposure for GCaMP7s and 50 ms exposure for GCaMP6f exposure) (F_0) were captured in the soma prior to glutamate uncaging, and 50 more frames were obtained after single photostimulation. The fractional change in fluorescence intensity relative to baseline ($\Delta F/F_0$) was calculated. The average peak amplitude in the control group was used to normalize the peak amplitude in each cell. The control group's average peak amplitude was compared to the experimental groups' average.

Reagents

Proteasome inhibitor MG132 (Allfa Aesar) was used at 10 μM to treat SH-SY5Y cells 4 hours before collecting whole cell lysates. 2 mM lithium chloride (LiCl) (Sigma-Aldrich) was used to inhibit GSK3β activity in SH-SY5Y cells and cultured cortical neurons, and 2 mM sodium chloride (NaCl) (Sigma-Aldrich) was used as a control. 2 μM tetrodotoxin (TTX) (Abcam) was used to block spontaneous Ca^{2+} activity in cultured cortical neurons. 1 μM 4-methoxy-7-

nitroindolinyl (MNI)-caged L-glutamate (Tocris Bioscience) was added to the culture media for glutamate uncaging.

Three-chamber test

To determine social behaviors, a three-chamber test was performed with a modification of the previously described method (48). The test animals' interaction with strangers was determined by the reciprocal sniffing time as described previously (56, 57). The test animals' interaction with a novel object was determined by the sniffing time that was defined as each instance in which a test mouse's nose was oriented in a 10-degree head orientation and comes within 2 cm toward a mouse or a wire cup as described previously (6). Before the test session, the subject mouse was placed in the center chamber and allowed to habituate for 5 minutes. Stranger mice were not habituated to apparatus. In the sociability test (10 minutes), an unfamiliar mouse (stranger 1) was placed in one side chamber under an inverted stainless-steel wire cup that allowed olfactory, visual, auditory, and tactile contacts, and an empty cup (a novel object) was placed in the opposite side chamber. During the social novelty test (10 minutes), a new unfamiliar mouse (stranger 2) was placed under a wire cup in the opposite side chamber that had been empty during the sociability phase. The subject mouse was allowed to explore freely in all 3 chambers during the tests. The behavior was recorded using a camera mounted overhead. The test animals' interaction with strangers was determined by the reciprocal sniffing time as described previously (56, 57). The test animals' interaction with a novel object was determined by the sniffing time that was defined as each instance in which a test mouse's nose was oriented in a 10-degree head orientation and comes within 2 cm toward a mouse or a wire cup as described previously (6). The discrimination index was calculated as (Total reciprocal sniffing time for stranger 1 – Total sniffing time for the object) / (Total reciprocal sniffing time for stranger 1 + Total sniffing time for the object) for the sociability test and (Total reciprocal sniffing

time for stranger 2 – Total reciprocal sniffing time for stranger 1) / (Total reciprocal sniffing time for stranger 2 + Total reciprocal sniffing time for stranger 1) for the social novelty test. We confirmed the reciprocal sniffing time manually and blindly by two different investigators.

Buried food assay

The buried food assay was performed as described previously (40). Several days before the test, 2-3 Froot Loops (Kellogg's) were placed in each cage overnight to confirm that the food is palatable to the mice. Mice that did not consume the Froot Loops were omitted from the test. Mice were food-deprived for 24 hours prior to the test. 2 Froot Loops were placed in a clean cage and buried under fresh bedding prior to placing the mice in the cage. Mice were allowed 20 minutes to explore the cage searching for the hidden food and the latency to find and begin to nibble on the food was recorded. Mice that did not find the food after 20 minutes were excluded from the results. The latency was blindly scored by two different investigators.

Open field test

We measured locomotor activity and anxiety-like behavior using the open field test as carried out previously (48). The test mouse was first placed in the center of the open field chamber (40 W x 40 L x 40 H cm) and was habituated to the apparatus for 5 minutes. Animals were then allowed to explore the chamber for 20 minutes. A 20 x 20 cm center square was defined as the inside zone. The behavior was recorded by a video camera. Data were analyzed using the ANY-maze tracking program to acquire total traveled distance (locomotor activity) and time spent outside and inside (anxiety-like behavior).

Statistical analysis

We used the GraphPad Prism 9 software to determine statistical significance (set at $p < 0.05$).

Grouped results of single comparisons were analyzed using the unpaired two-tailed Student's t-test. Differences between multiple groups were assessed by Two-way analysis of variance (ANOVA) with the Tukey test or nonparametric Kruskal-Wallis test with the Dunn's test. The graphs were presented as mean ± Standard Deviation (SD).

RESULTS

The δ-catenin G34S mutation increases GSK3β-mediated δ-catenin degradation.

GSK3β has previously been shown to act on δ-catenin via phosphorylation of threonine 1078 (T1078), which leads to ubiquitination and subsequent degradation of δ-catenin via proteosome (29, 48, 49). Conversely, inhibition of GSK3β has been shown to increase δ-catenin. Another relative of the armadillo protein repeat family, β-catenin also possess sites for phosphorylation by GSK3β toward the amino-terminus at serine 33 and 37 (S33 and S37), and threonine 41(T41) (50, 51). This GSK3β-mediated phosphorylation of β-catenin results in a similar fate to δ-catenin, with ubiquitination and proteasomal degradation (52) (**Fig 2**.). The significance of the β-catenin site of phosphorylation is that the Group-based Prediction System (53) predicts that the G34S mutation at the amino-terminus end of δ-catenin could mimic one of the β-catenin phosphorylation sites, potentially resulting in increased phosphorylation and degradation of G34S δ-catenin (**Fig 2.**).

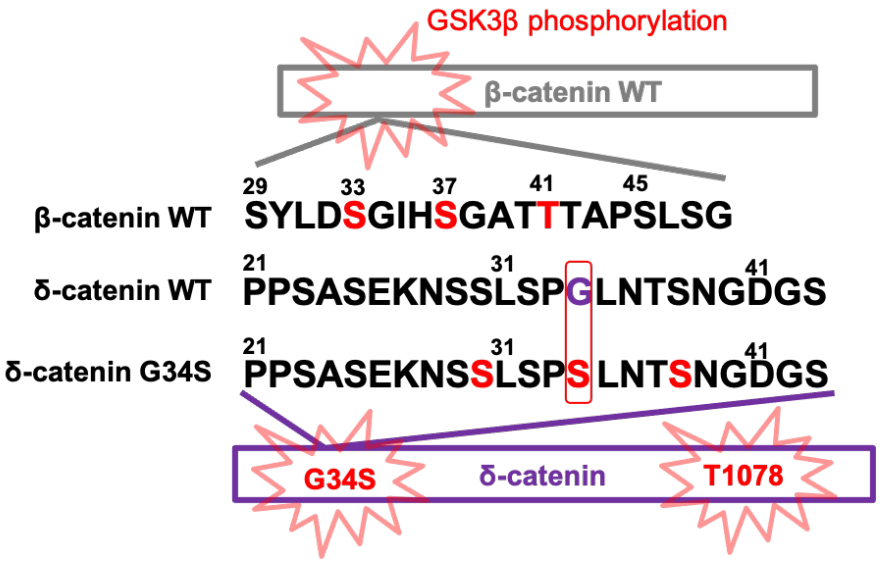

Figure 2. Amino acid sequence homology of β-catenin, WT δ-catenin and G34S δ-catenin. The δ-catenin G34S mutation adds an additional GSK3β-mediated phosphorylation site to induce δ-catenin degradation. GSK3β phosphorylation sites of β-catenin in the amino-terminal region known to induce proteasomal degradation of β-catenin highlighted in red (S33, S37, and T41) are comparable to possible GSK3β phosphorylation sites in the amino-terminus of G34S mutant δ-catenin also highlighted in

red (S30, S34, and S38). In addition to GSK3β-mediated threonine 1078 phosphorylation site in the carboxyl-terminus of δ-catenin, these potential amino-terminal GSK3β-mediated phosphorylation sites may enhance δ-catenin degradation.

To investigate the relationship between the δ-catenin G34S mutation and GSK3β-mediated degradation, we expressed wild-type WT or G34S δ-catenin in human neuroblastoma cells (SH-SY5Y) and compared levels of δ-catenin via immunoblotting. Normalize to WT δ-catenin levels, G34S δ-catenin levels were found to be significantly decreased (WT, 1.000 ± 0.286 and G34S, 0.592 ± 0.260, $p = 0.0227$) (**Fig. 3**).

Previous work has shown that LiCl treatment can significantly inhibit GSK3β activity and increase δ-catenin levels in culture neurons and mouse brains (21).To examine whether GSK3β mediates the loss of G34S δ-catenin, we used lithium chloride (LiCl) to pharmacologically inhibit GSK3β activity. WT or G34S δ-catenin was expressed in human neuroblastoma cells (SH-SY5Y) which are devoid of endogenous δ-catenin. These cells were then treated with 2 mM lithium chloride (LiCl) or sodium chloride (NaCl) for 18 hours prior to cell collection and lysing. We found that G34S δ-catenin levels were markedly reduced without LiCl (WT + NaCl, 1.000 ± 0.287 and G34S + NaCl, 0.479 ± 0.208, $p = 0.0354$) (**Fig. 3a**). Cells treated with LiCl showed significantly elevated levels of both WT and G34S δ-catenin (WT + LiCl, 1.456 ± 0.479, $p = 0.0300$, and G34S + LiCl, 1.336 ± 0.560, $p < 0.0001$) (**Fig. 3a**). To demonstrate that the LiCl treatment was sufficient to reduced GSK3β activity, we used immunoblotting to show that LiCl treated cells exhibited an increase in phosphorylation of GSK3β serine 9, which is the inactive form of GSK3β (58, 59) (21) (WT + NaCl, 1.000 ± 0.405 and WT + LiCl, 1.712 ± 0.644, $p = 0.0051$, and G34S + NaCl, 1.124 ± 0.433 and G34S + LiCl, 1.749 ± 0.635, $p = 0.0265$) (**Fig. 3a**).

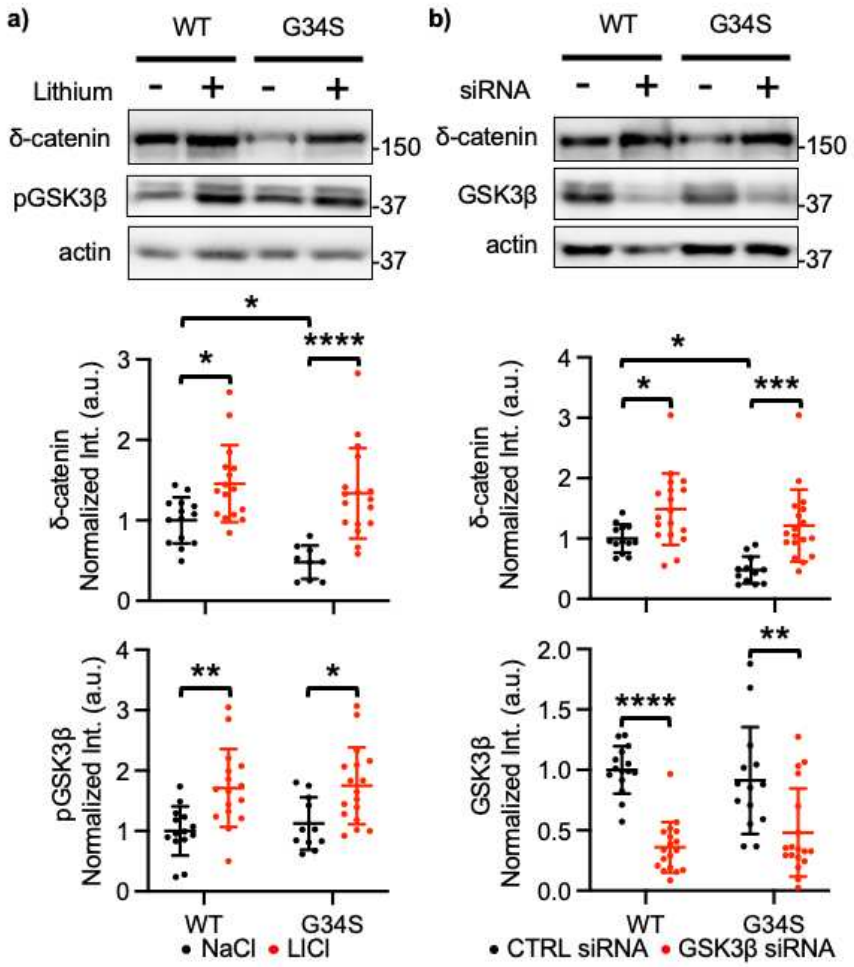

Figure 3. The δ-catenin G34S mutation increases GSK3β-mediated δ-catenin degradation. **a)** Representative immunoblots and summary graphs of normalized δ-catenin and pGSK3β levels in SH-SY5Y cell lysates transfected with WT or G34S δ-catenin and treated with 2 mM NaCl (-) or 2 mM LiCl (+) (n = number of immunoblots from 5 independent cultures. For δ-catenin, WT + NaCl = 14, WT + LiCl = 16, G34S + NaCl = 9, and G34S + LiCl = 17. For pGSK3β, WT + NaCl = 14, WT + LiCl = 16, G34S + NaCl = 11, and G34S + LiCl = 17. Two-way ANOVA with the Tukey test, *$p < 0.05$, **$p < 0.01$, and ****$p < 0.0001$). **b)** Representative immunoblots and summary graphs of normalized δ-catenin and GSK3β levels in SH-SY5Y cell lysates transfected with WT or G34S δ-catenin and treated with scrambled (CTRL) (-) or GSK3β (+) siRNA (n = number of immunoblots from 5 independent cultures. For δ-catenin, WT + CTRL siRNA = 13, WT + GSK3β siRNA = 18, G34S + CTRL siRNA = 12, and G34S + GSK3β siRNA = 18. For GSK3β, WT + CTRL siRNA = 15, WT + GSK3β siRNA = 18, G34S + CTRL siRNA = 14, and G34S + GSK3β siRNA = 18. Two-way ANOVA with the Tukey test, *$p < 0.05$, **$p < 0.01$, ***$p < 0.001$, and ****$p < 0.0001$). The position of molecular mass markers (kDa) is shown on the right of the blots. Conducted by Kaila Nip.

To account for potential off-target effects of the lithium treatment, we used siRNA to genetically inhibit GSK3β. The SH-SY5Y cells expression either WT or G34S δ-catenin were treated with either 25 nM scrambled siRNA (CTRL) or 25 nM GSK3β siRNA for 72 hours prior to

collection. When compared to WT δ-catenin, G34S δ-catenin levels in cells treated with the control siRNA was significantly reduced (WT + CTRL siRNA, 1.000 ± 0.231 and G34S + CTRL siRNA, 0.478 ± 0.223, $p = 0.0429$) (**Fig. 3b**). Both WT and G34S δ-catenin were significantly increased in cell that were treated with GSK3β siRNA (WT + GSK3β siRNA, 1.485 ± 0.592, $p = 0.0365$, and G34S + GSK3β siRNA, 1.215 ± 0.596, $p = 0.0007$) (**Fig. 3b**) We confirmed that GSK3β siRNA-mediated knockdown resulted in significantly reduced GSK3β levels, indicating a decrease in GSK3β activity (WT + CTRL siRNA, 1.000 ± 0.196 and WT + GSK3β siRNA, 0.359 ± 0.208, $p < 0.0001$, and G34S + CTRL siRNA, 0.912 ± 0.442 and G34S + GSK3β siRNA, 0.481 ± 0.365, $p = 0.0017$) (**Fig. 3b**).

To inspect the role of proteasomal degradation in the decreased levels of δ-catenin, we treated the cells with 10μM MG132, a proteasome inhibitor, for four hours and measured δ-catenin levels with immunoblotting. Inhibition of proteosome activity via MG132 resulted in a significant increase in both WT and G34S δ-catenin WT + MG132, 2.659 ± 1.630, $p = 0.0066$, and G34S + MG132, 2.239 ± 1.658, $p = 0.0002$), indicating that the degradation of δ-catenin due to GSK3β phosphorylation is mediated proteasomal degradation. **(Fig. 4)**

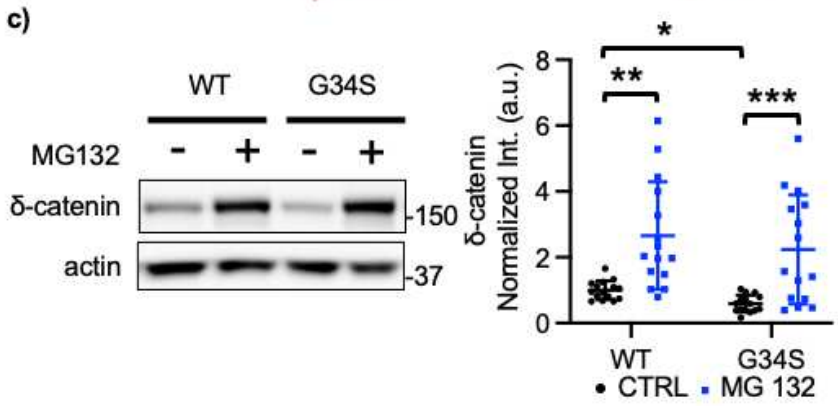

Figure 4. Proteasomal degradation enhances G34S δ-catenin degradation.
Representative immunoblots and summary graphs of normalized δ-catenin levels in SH-SY5Y cell lysates transfected with WT or G34S δ-catenin in the presence (+) or absence (-) of 10 μM MG132 (n = 15 immunoblots from 5 independent cultures, *p < 0.05, **p < 0.01, and ***p < 0.001, Kruskal-Wallis test with the Dunn's test). The position of molecular mass markers (kDa) is shown on the right of the blots. Conducted by Kaila Nip.

Altogether, we found that the δ-catenin G34S mutation causes increased GSK3β-mediated degradation via a proteasome-mediated mechanism, which we believe leads to a loss of δ-catenin function.

Additional δ-catenin mutations further confirm enhanced GSK3β-dependent δ-catenin degradation in the G34S mutation.

To gain a better understanding of the role of the glycine at residue 34 of δ-catenin we generated additional δ-catenin mutants. We generated a mutant with glycine 34 substituted for alanine (A), which is unable to be phosphorylated by GSK3β. Additionally, we generated a second new mutant where we substituted glycine 34 with aspartate (D) with assumes a phosphor-mimetic state. Each of these new mutants (G34A and G34D) as well as WT and G34S were each expressed in SH-SY5Y cells and δ-catenin levels were assessed using immunoblotting. We found no significant difference between WT δ-catenin and G34A δ-catenin expression, and G34D δ-catenin was found to be significantly reduced as compared to WT and G34A δ-catenin (WT, 1,000, G34A, 1.311 ± 0.437, and G34D, 0.662 ± 0.150, WT vs. G34A, $p > 0.999$, WT vs. G34D, $p = 0.0088$, G34A vs. G34D, $p = 0.0088$) similarly to cells expressing the G34S δ-catenin mutant (**Fig. 5a**). To determine whether GSK3β-mediated phosphorylation of G34S δ-catenin is necessary for increased degradation of δ-catenin, we initially used LiCl to pharmacologically inhibit GSK3β activity. Since we established the similarities between WT and G34A δ-catenin, we expressed either G34A or G34D in SH-SY5Y cell and then treated them with 2mM LiCl or 2mM NaCl for 18 hours prior to collection. We found that in the absence of LiCl, G34D δ-catenin was significantly reduced as compared to G34A δ-catenin (G34A + NaCl, 1.000 ± 0.258 and G34D + NaCl, 0.551 ± 0.361, $p = 0.0101$) (**Fig. 5a**). LiCl treatment was found to raise the level of G34A δ-catenin, but not G34D δ-catenin (G34A + LiCl, 1.583 ± 0.458, $p = 0.0005$, and G34D + LiCl, 0.476 ± 0.255, $p = 0.9433$) (**Fig. 5a**). Additionally, we confirmed that

the LiCl treatment significantly increased the inactive form of GSK3β, pGSK3β, indicating GSK3β was inhibited (G34A + NaCl, 1.000 ± 0.197 and G34A + LiCl, 1.601 ± 0.531, $p = 0.0317$, and G34D + NaCl, 0.982 ± 0.245 and G34D + LiCl, 1.557 ± 0.877, $p = 0.0372$) (**Fig. 5b**). We again used GSK3β siRNA for genetic inhibition of GSK3β activity. The G34A δ-catenin or G34D mutant δ-catenin was expressed in SH-SY5Y cells with either 25 nM scrambled siRNA (CTRL) or 25 nM GSK3β siRNA for 72 hours prior to collection. Comparison of G34A δ-catenin and G34D δ-catenin levels in cells treated with scrambled siRNA showed significantly reduced δ-catenin G34D levels as compared to G34A δ-catenin (G34A + CTRL siRNA, 1.000 ± 0.166 and G34D + CTRL siRNA, 0.393 ± 0.230, $p = 0.0330$) (**Fig. 5c**). GSK3β knockdown, like the LiCl treatment had no effect on G34D δ-catenin levels but was able to increase G34A δ-catenin expression (G34A + GSK3β siRNA, 2.100 ± 0.841, $p < 0.0001$, and G34D + GSK3β siRNA, 0.594 ± 0.424, $p = 0.8190$) (**Fig. 5c**). Additionally, GSK3β siRNA knockdown significantly decreased GSK3β levels (G34A + CTRL siRNA, 1.000 ± 0.388 and G34A + GSK3β siRNA, 0.467 ± 0.137, $p = 0.0171$, and G34D + CTRL siRNA, 1.218 ± 0.599 and G34D + GSK3β siRNA, 0.479 ± 0.189, $p = 0.0013$) (**Fig. 5c**). Taken together, these finding suggest that the glycine to serine mutation at residue 34 of δ-catenin is necessary for the enhanced GSK3β-mediated δ-catenin degradation, which is likely the cause of the loss of δ-catenin function.

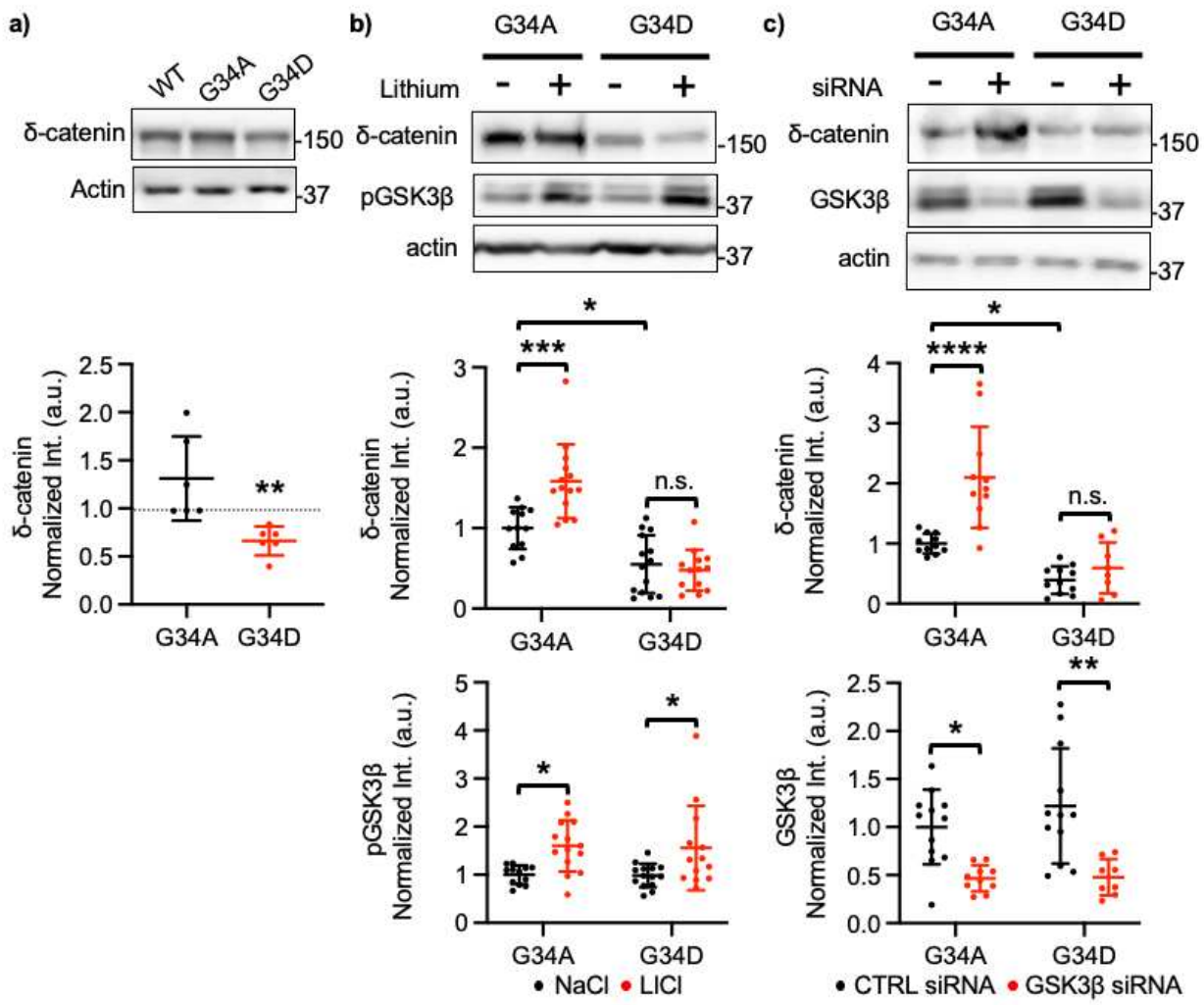

Figure 5. Additional δ-catenin mutations confirm enhanced GSK3β-dependent δ-catenin degradation in the G34S mutation.

a) Representative immunoblots and summary graphs of normalized δ-catenin levels in SH-SY5Y cell lysates transfected with WT, G34A, or G34D δ-catenin (n = 6 immunoblots from 3 independent cultures, Kruskal-Wallis test with the Dunn's test, **p < 0.01). **b)** Representative immunoblots and summary graphs of normalized δ-catenin and pGSK3β levels in SH-SY5Y cell lysates transfected with G34A or G34D δ-catenin and treated with 2 mM NaCl (-) or 2 mM LiCl (+) (n = number of immunoblots from 3 independent cultures. G34A + NaCl = 12, G34A + LiCl = 14, G34D + NaCl = 14, and G34D + LiCl = 13. Two-way ANOVA with the Tukey test, *p < 0.05 and ***p < 0.001. n.s. indicates no significant difference). **c)** Representative immunoblots and summary graphs of normalized δ-catenin and GSK3β levels in SH-SY5Y cell lysates transfected with WT or G34S δ-catenin and treated with scrambled (CTRL) (-) or GSK3β (+) siRNA (n = number of immunoblots from 3 independent cultures. For δ-catenin, G34A + CTRL siRNA = 11, G34A + GSK3β siRNA = 11, G34D + CTRL siRNA = 11, and G34D + GSK3β siRNA = 8. For GSK3β, G34A + CTRL siRNA = 12, G34A + GSK3β siRNA = 10, G34D + CTRL siRNA = 12, and G34D + GSK3β siRNA = 8. Two-way ANOVA with the Tukey test, *p < 0.05, **p < 0.01, and ****p < 0.0001. n.s. indicates no significant difference). The position of molecular mass markers (kDa) is shown on the right of the blots. Conducted by Kaila Nip.

Lithium treatment reverses the reduction of synaptic δ-catenin and GluA2 in the G34S δ-catenin cortex.

To better understand the mechanism by which the G34S mutation affects δ-catenin and AMPAR levels in vivo, we used a δ-catenin G34S knock-in mouse line that was generated at University of Nebraska Medical Center (UNMC) Mouse Genome Engineering Core utilizing the CRISPR-Cas9 technique (60). We collected whole tissue lysates and post synaptic density (PSD) fraction from the cortices of 3-month-old male and female WT and G34S mutant animals to assess both total and synaptic levels of δ-catenin via immunoblotting. In whole tissue lysates, we found a significant decrease in the total δ-catenin levels in the cortex of male G34S mutants as compared to the cortical levels of δ-catenin in male WT littermates (WT male, 1.000 ± 0.608 and G34S male, 0.318 ± 0.206, $p = 0.0035$). Interestingly, the whole tissue cortical lysates of female G34S mice showed no total difference in δ-catenin levels as compared to their female WT littermates (WT female, 1.000 ± 0.406 and G34S female, 0.960 ± 0.294, $p = 0.8056$) (**Fig. 4**). Moreover, we found no difference total cortical GluA1 (WT female, 1.000 and G34S female, 0.943 ± 0.619, $p = 0.4723$, WT male 1.000, and G34S male, 0.848 ± 0.206, $p = 0.3362$) or GluA2 (WT female 1.000 and G34S female, 0.943 ± 0.619, $p = 0.4723$, WT male, 1.000 and G34S male, 0.848 ± 0.206, $p = 0.3362$) levels between WT and G34S males or females (**Fig. 6**)

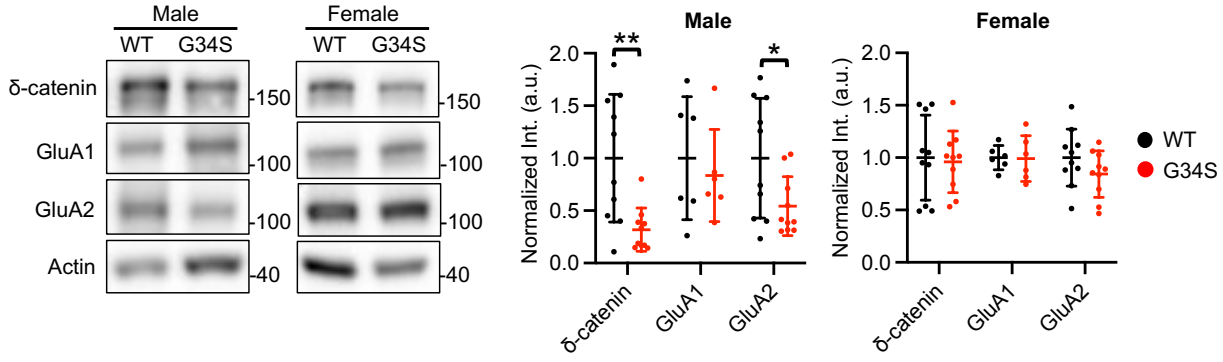

Figure 6. Total δ-catenin and AMPAR levels in the cortex of WT and δ-catenin G34S mice. Representative immunoblots and summary graphs of normalized total δ-catenin, GluA1, and GluA2 levels in the male and female whole tissue lysates from WT and δ-catenin G34S mice showing a reduction of total δ-catenin and GluA2 in the G34S male cortex compared to the WT male cortex, while no difference in total δ-catenin and GluA2 levels between the WT and G34S female cortex (n = 10 immunoblots from 4

mice in each condition, *$p < 0.05$ and **$p < 0.01$, the unpaired two-tailed Student's t-test). There is no difference in total GluA1 (n = 6 immunoblots from 4 mice in each condition) levels between the WT and G34S male and female cortex. The position of molecular mass markers (kDa) is shown on the right of the blots.

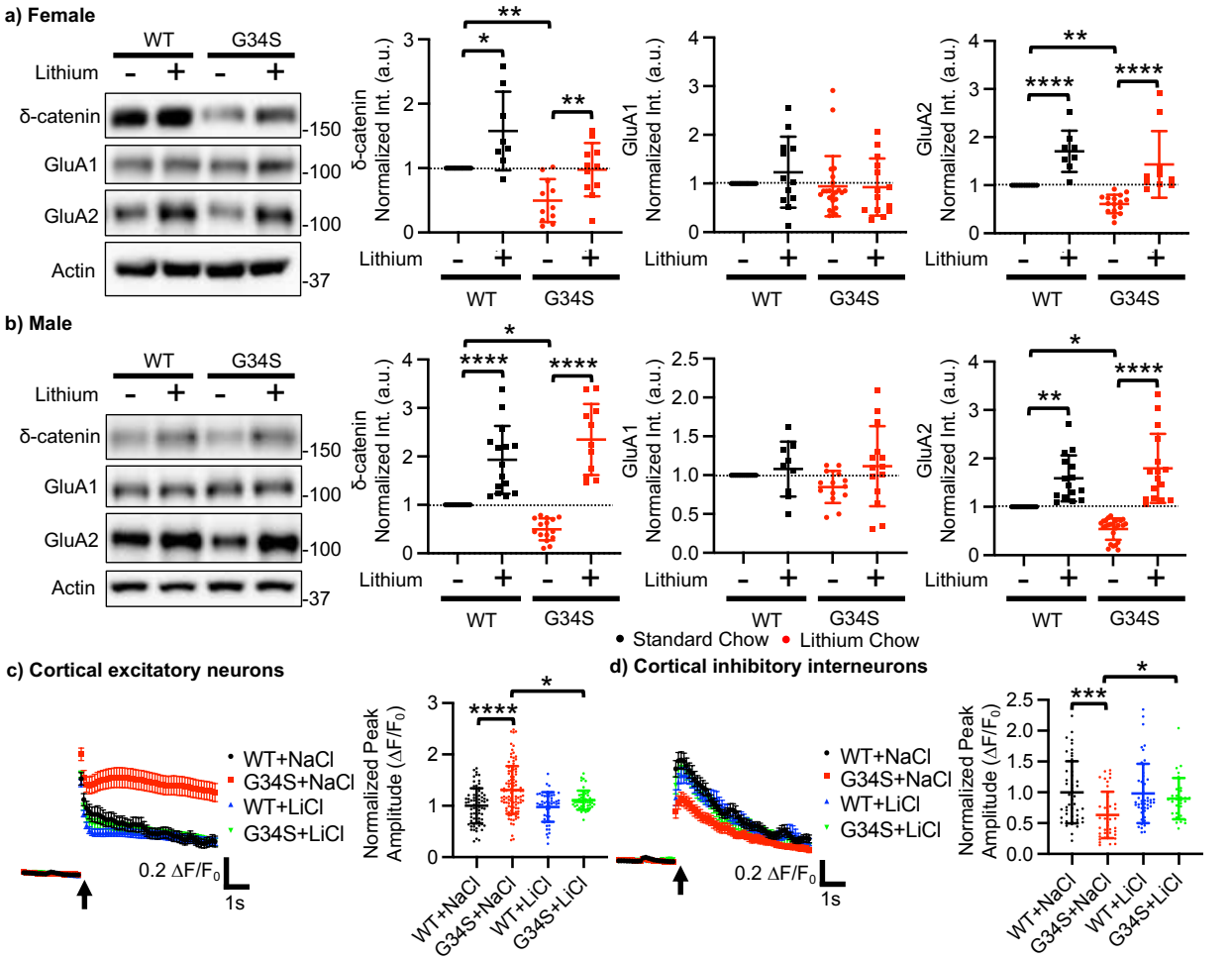

Figure 7. Lithium treatment reverses a significant reduction of synaptic δ-catenin and GluA2 in the δ-catenin G34S cortex and alterations in glutamatergic activity in cultured cortical neurons. Representative immunoblots and summary graphs of normalized δ-catenin, GluA1, and GluA2 levels in the cortical PSD fractions from standard chow (-) or lithium chow (+)-fed WT and δ-catenin G34S **a)** female (n = number of immunoblots [number of mice]. For δ-catenin, WT + standard chow =14 [5], WT + lithium chow = 8 [5], G34S + standard chow = 11 [6], and G34S + lithium chow = 11 [6]. For GluA1, WT + standard chow = 14 [5], WT + lithium chow = 12 [5], G34S + standard chow = 23 [6], and G34S + lithium chow = 14 [6]. For GluA2, WT + standard chow = 11 [5], WT + lithium chow = 8 [5], G34S + standard chow = 16 [6], and G34S + lithium chow = 10 [6]) and **b)** male mice (n = number of immunoblots [number of mice]. For δ-catenin, WT + standard chow = 17 [5], WT + lithium chow = 15 [5], G34S + standard chow = 15 [6], and G34S + lithium chow = 11 [6]. For GluA1, WT + standard chow = 14 [5], WT + lithium chow = 9 [5], G34S + standard chow = 14 [6], and G34S + lithium chow = 14 [6]. For GluA2, WT + standard chow = 18 [5], WT + lithium chow = 15 [5], G34S + standard chow = 24 [6], and G34S + lithium chow = 15 [6], *$p < 0.05$, **$p < 0.01$, and ****$p < 0.0001$, Two-way ANOVA with the Tukey test). The position of molecular mass markers (kDa) is shown on the right of the blots. **c)** Average traces of GCaMP7s signals and summary data of normalized peak amplitude in each condition in excitatory neurons (n = number of neurons from 3 independent cultures, WT + NaCl = 75, G34S + NaCl = 98, WT + LiCl = 50, and G34S +

LiCl = 49). **d)** Average traces of GCaMP6f signals and summary data of normalized peak amplitude in each condition in inhibitory interneurons (n = number of neurons from 3 independent cultures, WT + NaCl = 46, G34S + NaCl = 40, WT + LiCl = 46, and G34S + LiCl = 31, *$p < 0.05$, ***$p < 0.01$, and ****$p < 0.0001$, Two-way ANOVA with the Tukey test). An arrow indicates photostimulation.

Focusing on synaptic δ-catenin levels, we found a significant decrease in the δ-catenin in cortical PSD fractions (WT female, 1.000 and G34S female, 0.494 ± 0.334, $p = 0.0070$, WT male, 1.000 and G34S male, 0.494 ± 0.227, $p = 0.0348$), as well as GluA2 levels (WT female 1.000 and G34S female, 0.612 ± 0.192, $p = 0.0017$, WT male, 1.000 and G34S male, 0.540 ± 0.222, $p = 0.0440$) in the cortex of male and female G34S δ-catenin mice as compared to the cortex of their WT littermates. Still, we found no difference in synaptic GluA1 levels (WT female 1.000 and G34S female, 0.943 ± 0.619, $p = 0.4723$, WT male, 1.000, and G34S male, 0.848 ± 0.206, $p = 0.3362$) in the cortex of G34S mutant animals as compared to their WT littermates (**Fig. 7a and 7b**).

Next, synaptic levels of δ-catenin, GluA1 and GluA2 in the hippocampus of WT and G34S mutant mice were also analyzed via immunoblotting. We found no difference in synaptic levels of δ-catenin (WT female, 1.000 and G34S female, 0.929 ± 0.222, $p = 0.4344$, and WT male, 1.000 and G34S male, 0.847 ± 0.371, $p = 0.4843$), GluA1 (WT female, 1.000 and G34S female, 1.293 ± 0.457, $p = 0.3876$, and WT male, 1.000 and G34S male, 0.880 ± 0.311, $p = 0.8050$), or GluA2 levels (WT female, 1.000 and G34S female, 0.931 ± 0.366, $p = 0.3654$, and WT male, 1.000 and G34S male, 0.848 ± 0.206, $p = 0.9672$) in the hippocampus of WT and G34S (**Fig. 8a**). This finding indicates that the G34S δ-catenin mutation results in a significant reduction of synaptic δ-catenin and GluA2 levels selectively, affecting the cortex, but not the hippocampus of G34S mutant animals. The differential effect of the G34S δ-catenin mutation may be due to the increased presence of GluA2 in the hippocampus as compared to the cortex, thus resulting in a stronger effect on the cortex than the hippocampus (55, 56).

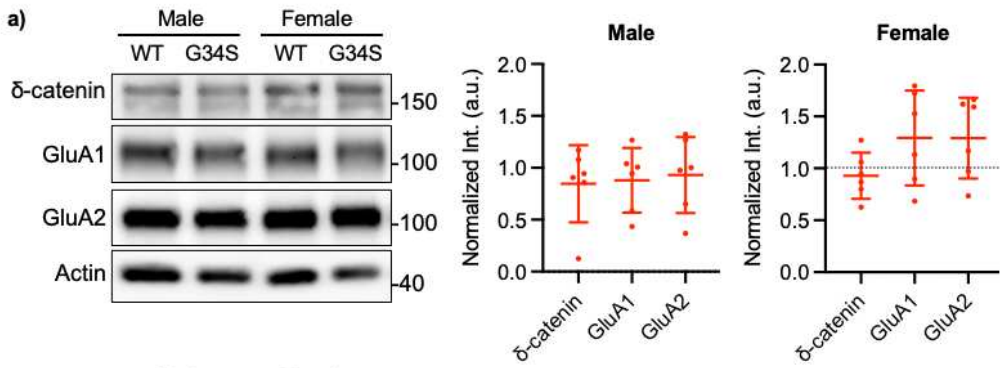

Figure 8. Synaptic δ-catenin and AMPAR levels in the hippocampus of G34S δ-catenin mice.
a) Representative immunoblots and summary graphs of normalized δ-catenin, GluA1, and GluA2 levels in the male and female hippocampal PSD fractions from WT and δ-catenin G34S showing no difference in synaptic δ-catenin and AMPAR levels between the WT and G34S hippocampus (n = 6 immunoblots from 3 mice in each condition, Kruskal-Wallis test with the Dunn's test). Work done by Matheus Sathler.

To investigate whether pharmacological inhibition of *in vivo* GSK3β activity via lithium treatment can reverse the effect of the G34S δ-catenin mutation on synaptic δ-catenin and AMPA receptor levels in the cortex. We treated 3-month-old female and male WT and G34S δ-catenin mutant mice with chow containing 0.17% w/w lithium carbonate *ad libitum* for 7 complete days prior to use. Following the lithium treatment, we collected whole tissue lysates of the cortex, and measured pGSK3β levels to determine if the lithium treatment was sufficient to inhibit GSK3β activity in the cortex of these animals. In the cortex of male and female G34S δ-catenin mutant animals, the lithium treatment increased pGSK3β, as compared to the controls which confirmed the adequacy of the treatment for in vivo inhibition of GSK3β (WT female + standard chow, 1.000 ± 0.311 and WT female + lithium chow, 1.495 ± 0.292, $p = 0.0175$, G34S female + standard chow, 1.024 ± 0.200 and G34S female + lithium chow, 1.481 ± 0.551, $p = 0.0222$, WT male + standard chow, 1.000 ± 0.118 and WT male + lithium chow, 1.455 ± 0.355, $p = 0.0087$, and G34S male + standard chow, 0.931 ± 0.347 and G34S male + lithium chow, 1.347 ± 0.314, $p = 0.0006$) (**Fig. 9a and 9b**).

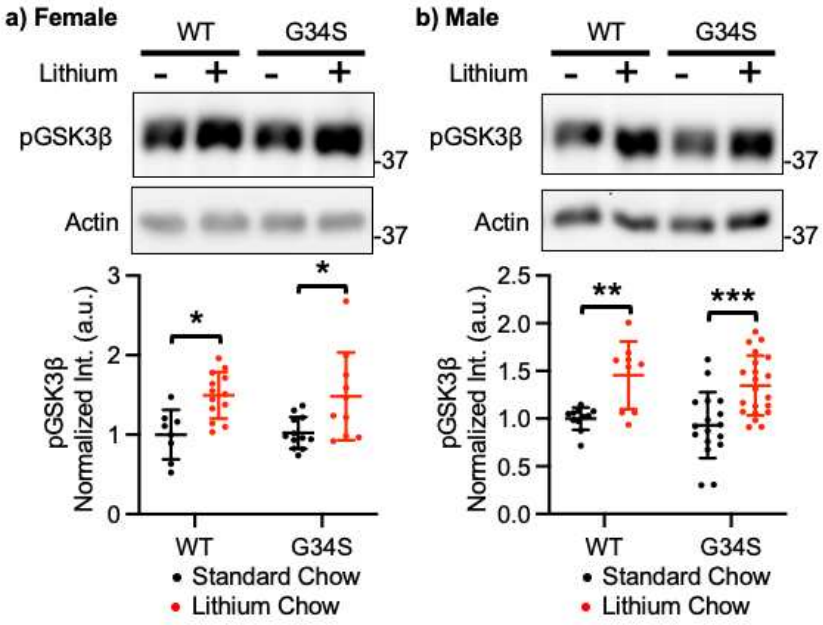

Figure 9. Lithium treatment significantly reduces in vivo GSK3β activity.
Representative immunoblots and summary graphs of normalized pGSK3β levels in the whole cell lysates from the cortex of standard chow (-) or lithium chow (+)-fed WT and δ-catenin G34S **a)** female (n=number of immunoblots [number of mice]. WT female + standard chow = 8 [6], WT female + lithium chow = 13 [6], G34S female + standard chow = 12 [6], and G34S female + lithium chow = 10 [6]) and **b)** male cortex (WT male + standard chow=11 [6], WT male + lithium chow = 9 [6], G34S male + standard chow = 17 [6], and G34S male + lithium chow = 21 [6]). *p < 0.05, **p < 0.01, and ***p < 0.001, Two-way ANOVA with the Tukey test). The position of molecular mass markers (kDa) is shown on the right of the blots.

We also collected cortical PSD fractions from the 3-month-old female and male WT and δ-catenin G34S animals following lithium treatment to determine if synaptic δ-catenin and GluA2 levels were affected by the inhibition of GSK3β activity. We found that the lithium treatment significantly increased synaptic δ-catenin (WT female + lithium chow, 1.578 ± 0.611, p = 0.0189, G34S female + lithium chow, 0.977 ± 0.414, p = 0.0088, WT male + lithium chow, 1.929 ± 0.699, p < 0.0001, and G34S male + lithium chow, 2.350 ± 0.734, p < 0.0001) as well as GluA2 levels (WT female + lithium chow, 1.705 ± 0.431, p < 0.0001, G34S female + lithium chow, 1.432 ± 0.693, p < 0.0001, WT male + lithium chow, 1.588 ± 0.476, p = 0.0016, and G34S male + lithium chow, 1.795 ± 0.714, p < 0.0001) in the male and female G34S δ-catenin mutant cortex (**Fig. 7a and 7b**). We found no difference in GluA1 levels (WT female + lithium chow, 1.232 ± 0.731, p = 0.7081, G34S female + lithium chow, 0.926 ± 0.587, p = 0.8723, WT male +

lithium chow, 1.078 ± 0.355, p = 0.7834, and G34S male + lithium chow, 1.116 ± 0.515, p = 0.0539) in WT and G34S mutant cortex following lithium treatment (**Fig. 7a and 7b**). Thus, our findings indicate that pharmacological inhibition of GSK3β activity via lithium is sufficient to increase the synaptic δ-catenin and GluA2 levels in the G34S δ-catenin mutant cortex.

Cultured G34S δ-catenin cortical neurons exhibit altered glutamatergic activity.

It has been previously established that ASD may be mediated by altered neuronal excitation and inhibition (E/I) balance (61). Maintaining an adequate balance in cellular E/I is also known to be essential for the function of normal social behavior (5). Moreover, postsynaptic glutamatergic activity in cortical excitatory or inhibitory neurons mediates social behavior via the regulation of neuronal E/I within neural network of the cortex (5, 11). A recent study found that δ-catenin deficiency causes an increased E/I ratio, and increases the intrinsic excitability of cortical excitatory neurons (26). Because our early findings showed that G34S δ-catenin cortex possessed decreased GluA2, we carried out Ca^{2+} imaging with glutamate uncaging in WT and G34S δ-catenin cultured cortical neurons to inspect the relationship between the G34S δ-catenin mutation and potentially alterations in glutamatergic activity in excitatory and inhibitory cells. We found that glutamatergic activity was significantly increased in G34S δ-catenin cultured excitatory cortical neurons (12-14 days *in vitro* (DIV)) as compared to WT cells (WT, 1.000 ± 0.340 $\Delta F/F_0$ and G34S, 1.307 ± 0.465 $\Delta F/F_0$, $p < 0.0001$) (**Fig. 7c**). Alternately, glutamatergic activity in cultured G34S δ-catenin inhibitory interneurons was distinctly lower when compared to the WT cells (WT, 1.000 ± 0.504 $\Delta F/F_0$ and G34S, 0.621 ± 0.360 $\Delta F/F_0$, p = 0.0005) (**Fig. 7d**).

As we had previously found that pharmacological inhibition of GSK3β activity is sufficient to restore normal synaptic levels of δ-catenin and GluA2 in the cortex of mutant animals, we endeavored to determine whether lithium treatment is sufficient to reverse the

observed alterations in glutamatergic activity in mutant neurons (**Fig. 7a and 7b**). We treated cultured cortical neurons with 2 mM LiCl for 4 hours then performed Ca^{2+} imaging with glutamate uncaging. Inhibition of GSK3β activity was found to reverse the effects of G34S δ-catenin on glutamatergic activity in cultured cortical excitatory (G34S, 1.109 ± 0.188 $\Delta F/F_0$, p = 0.0109) and inhibitory cells (G34S, 0.898 ± 0.334 $\Delta F/F_0$, $p < 0.0419$) (**Fig. 7c and 7d**). Lithium treatment of WT neurons showed no effect on glutamatergic activity (Excitatory neurons, WT + LiCl, 0.978 ± 0.290 $\Delta F/F_0$, p = 0.9869, and inhibitory interneurons, WT + LiCl, 0.982 ± 0.481 $\Delta F/F_0$, p = 0.9973) (**Fig. 7c and 7d**). Altogether, our findings demonstrate that the G34S δ-catenin mutant causes significant alteration of AMPAR-mediated glutamatergic activity which differentially effects excitatory and inhibitory cells. We believe this effect likely disrupts neuronal E/I balance in the cortex . Moreover, we discovered that these changes in G34S mutant neurons can be reversed by pharmacological inhibition of GSK3β activity.

δ-catenin G34S induces social dysfunction in mice, reversible by GSK3β inhibition.

We preformed the three-chamber test to determine whether the G34S δ-catenin mutation influences social behavior in mutant animals. We found that WT male and female mice exhibited normal sociability preference as they were observed to interact significantly longer with stranger 1 than the novel object during the sociability portion of the test (**Fig. 10a and Table 1**). Conversely, δ-catenin G34S male and female mice demonstrated a significantly low preference to socialize as they exhibited no preference for social interaction over interaction with a novel object, resulting in a similar total interaction time between stranger 1 and the novel object (**Fig. 10a and Table 1**). Moreover, the G34S δ-catenin male and female mice interacted significantly less with stranger 1 than WT mice (**Fig. 10a and Table 1**). In the social novelty portion of the test, WT mice demonstrated normal social novelty preference, and engaged with stranger 2 for longer than they did with stranger 1 (**Fig. 10b and Table 1**). However, the G34S

δ-catenin male and female mice showed no significant difference in reciprocal sniffing time between stranger 1 and stranger 2 in (**Fig. 10b and Table 1**). Compared to WT mice, G34S δ-catenin male and female mice exhibited significantly decreased social interaction time with stranger 2 (**Fig. 10b and Table 1**). These findings indicate that G34S δ-catenin mice exhibit both disrupted sociability preference and disrupted preference for social novelty.

Because we found that lithium treatment significantly reduces GSK3β activity and was sufficient to elevate synaptic δ-catenin and GluA2 levels in the G34S δ-catenin cortex (**Fig. 7**), we endeavored to determine if lithium treatment would be sufficient to restore normal social behavior in the mutant mice. In the sociability test, we discovered that when fed with lithium chow, WT and G34S δ-catenin male and female mice spent a greater amount of time interacting with stranger 1 than with the novel object. This finding strongly indicates that inhibition of GSK3β activity is sufficient for reversing both the synaptic δ-catenin and GluA2 deficiencies and the disrupted sociability preference in G34S δ-catenin mice (**Fig. 10a and Table 1**). Moreover, we found that when on lithium treatment, G34S δ-catenin mice showed significantly increased social interaction time with stranger 1 in the sociability portion of test as compared to those without lithium treatment (**Fig. 10a and Table 1**).

We also found that both lithium-fed WT and G34S δ-catenin male and female mice interacted significantly longer with stranger 2 than stranger 1 during the social novelty portion of the test, demonstrating that lithium treatment is sufficient to restore normal social novelty preference in the G34S δ-catenin mice (**Fig. 10b and Table 1**). Additionally, δ-catenin G34S mice showed a significant increase in social interaction time with stranger 2 when treated with lithium (**Fig. 10b and Table 1**). Taken all together, we found that the G34S δ-catenin mutation causes impaired social behavior in mice, which can be reversed by the lithium-based pharmacological inhibition of *in vivo* GSK3β activity.

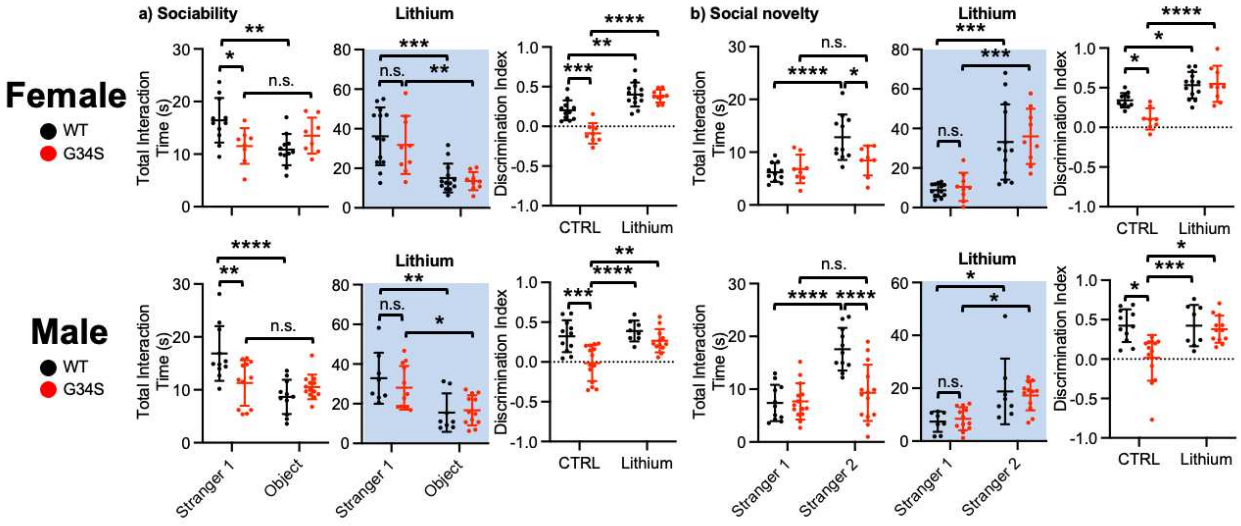

Figure 10. δ-catenin G34S induces social dysfunction in mice, which is reversed by GSK3β inhibition.
Total interaction time and the discrimination index of **a)** sociability and **b)** social novelty in female and male mice in each genotype in control and lithium treated conditions (highlighted in light blue) in the three-chamber test (n = number of animals, WT female + standard chow = 11, WT female + lithium chow = 9, G34S female + standard chow = 8, G34S female + lithium chow = 7, WT male + standard chow =11, WT male + lithium chow = 8, G34S male + standard chow = 14, and G34S male + lithium chow = 12, *p < 0.05, **p < 0.01, ***p < 0.001, and ****p < 0.0001, Two-way ANOVA with Tukey test. n.s. indicates no significant difference).

Table 1. Three-chamber test summary of WT and G34S mice with regular and lithium chow.

Regular chow									
Female	WT (n = 11 mice)		G34S (n = 8 mice)		Male	WT (n = 11 mice)		G34S (n = 14 mice)	
Sociability	Stranger 1	Objective	Stranger 1	Objective	Sociability	Stranger 1	Objective	Stranger 1	Objective
Total Interaction Time (sec)	16.445 ± 4.244	10.855 ± 2.973	11.538 ± 3.387	13.513 ± 3.433	Total Interaction Time (sec)	16.864 ± 5.169	8.655 ± 3.244	10.986 ± 4.035	10.829 ± 2.691
	Stranger 1 vs. Objective, p = 0.0042		Stranger 1 vs. Objective, p = 0.3888			Stranger 1 vs. Objective, p < 0.0001		Stranger 1 vs. Objective, p = 0.9995	
	WT Stranger 1 vs. G34S Stranger 1, p = 0.0268					WT Stranger 1 vs. G34S Stranger 1, p = 0.0023			
Social novelty	Stranger 1	Stranger 2	Stranger 1	Stranger 2	Social novelty	Stranger 1	Stranger 2	Stranger 1	Stranger 2
Total Interaction Time (sec)	6.182 ± 1.795	12.827 ± 4.303	6.825 ± 2.712	8.425 ± 2.843	Total Interaction Time (sec)	7.391 ± 3.428	17.573 ± 4.037	7.679 ± 9.314	9.314 ± 5.332
	Stranger 1 vs. 2, p < 0.0001		Stranger 1 vs. 2, p = 0.7307			Stranger 1 vs. 2, p < 0.0001		Stranger 1 vs. 2, p = 0.7297	
	WT Stranger 2 vs. G34S Stranger 2, p = 0.0212					WT Stranger 2 vs. G34S Stranger 2, p < 0.0001			

Lithium chow									
Female	WT (n = 13 mice)		G34S (n = 9 mice)		Male	WT (n = 8 mice)		G34S (n = 12 mice)	
Sociability	Stranger 1	Objective	Stranger 1	Objective	Sociability	Stranger 1	Objective	Stranger 1	Objective
Total Interaction Time (sec)	36.192 ± 14.596	15.069 ± 7.317	31.800 ± 14.691	13.544 ± 4.571	Total Interaction Time (sec)	32.850 ± 12.862	15.500 ± 9.699	28.042 ± 10.979	16.667 ± 7.563
	Stranger 1 vs. Objective, $p = 0.0001$		Stranger 1 vs. Objective, $p = 0.0074$			Stranger 1 vs. Objective, $p = 0.0089$		Stranger 1 vs. Objective, $p = 0.0468$	
	WT Stranger 1 vs. G34S Stranger 1, $p = 0.8061$					WT Stranger 1 vs. G34S Stranger 1, $p = 0.7336$			
Social novelty	Stranger 1	Stranger 2	Stranger 1	Stranger 2	Social novelty	Stranger 1	Stranger 2	Stranger 1	Stranger 2
Total Interaction Time (sec)	8.746 ± 3.242	33.154 ± 19.031	10.433 ± 7.117	35.989 ± 13.988	Total Interaction Time (sec)	7.363 ± 3.864	18.800 ± 12.404	8.450 ± 4.345	17.258 ± 5.579
	Stranger 1 vs. 2, $p < 0.0001$		Stranger 1 vs. 2, $p = 0.0006$			Stranger 1 vs. 2, $p = 0.0117$		Stranger 1 vs. 2, $p = 0.0182$	
	WT Stranger 2 vs. G34S Stranger 2, $p = 0.9550$					WT Stranger 2 vs. G34S Stranger 2, $p = 0.9615$			

G34S δ-catenin mice exhibit normal olfaction, anxiety levels, and locomotor activity.

Sensory deficits are known to affect performance in social behavioral assays and olfaction is critically important for social activity in mice (62). The buried food assay is a reliable method that tests a mouse's olfaction by exploiting their natural desire to forage using olfactory cues (63). Thus, we conducted the buried food test to examine if the G34S δ-catenin mutation could affect or impair olfactory functions. We found that the G34S δ-catenin male and female mice show no significant difference in the latency to find the buried food as compared to their WT littermates, indicating that G34S δ-catenin mice exhibit normal olfactory function (**Fig. 11a and Table 2**). Similarly, anxiety levels can also negatively impact social behavior in animals (64, 65). Thus, we assessed anxiety-like behavior and locomotor activity using an open field test. We found no difference between WT and G34S δ-catenin mice regardless of sex in total traveled distance (locomotor activity) and time spent on the outside (anxiety-like behavior) and inside areas of the open field chamber (**Fig. 11b and Table 2**). This finding demonstrates that G34S δ-catenin mice exhibit normal locomotor activity and anxiety levels. Taken together, G34S δ-

catenin mice show normal olfaction, locomotion and anxiety-like behavior, indicating that the altered behaviors observed in the three-chamber test (**Fig. 11a**) strongly indicate social dysfunction.

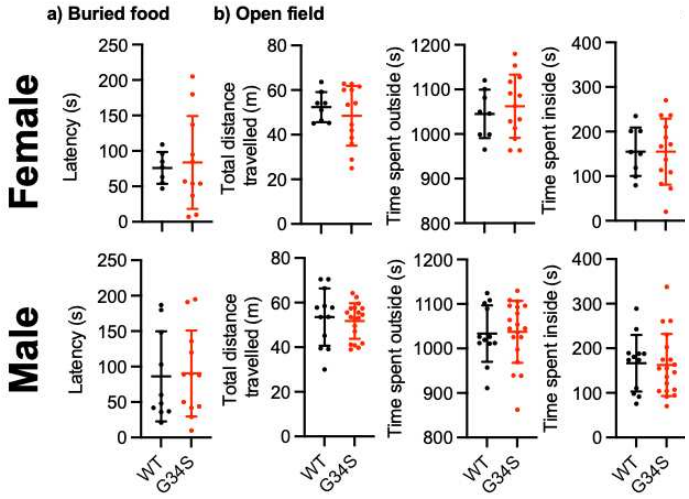

Figure 11. Normal olfaction, locomotor activity, and anxiety levels in δ-catenin G34S mice. The results of the buried food test showing normal olfaction in δ-catenin G34S **a)** females (n = 7 WT and 11 G34S mice) and males (n = 10 WT and 12 G34S mice). **b)** The results of the open field test measuring total distance travelled and time spent outside and inside showing normal locomotor activity and no anxiety-like behavior in δ-catenin G34S females (n = 8 WT and 13 G34S mice) and males (n = 12 WT and 19 G34S mice).

Table 2. Summary of the buried food and open field tests.

	Buried food test	Open field test		
Female	The latency (Seconds)	Total distance travelled (m)	Total time spent outside (Seconds)	Total time spent inside (Seconds)
WT	76.000 ± 22.443	52.378 ± 6.751	1045.150 ± 54.380	154.850 ± 54.380
G34S	83.727 ± 65.521	48.454 ± 13.409	1062.338 ± 70.804	154.892 ± 73.942
	p = 0.7694	p = 0.4537	p = 0.5645	p = 0.9988
Male	The latency (Seconds)	Total distance travelled (m)	Total time spent outside (Seconds)	Total time spent inside (Seconds)
WT	86.200 ± 63.554	53.532 ± 12.868	1033.308 ± 63.382	166.692 ± 63.382
G34S	90.333 ± 60.593	51.742 ± 7.954	1037.368 ± 69.715	162.632 ± 69.715
	p = 0.8777	p = 0.6346	p = 0.8713	p = 0.8623

δ-catenin KO mice exhibit abnormal social behavior.

We used the three-chamber test to determine whether the absence of δ-catenin expression effects social behavior in δ-catenin KO mice. In the sociability portion of the test, WT male and female mice demonstrated normal sociability and interacted significantly longer with stranger 1 than a novel object (**Fig. 12a and Table 3**). However, δ-catenin KO male and female mice showed no significant difference in total interaction time between stranger 1 and the novel object, indicating impaired sociability preference (**Fig. 12a and Table 3**). Significantly, δ-catenin KO male and female mice engaged in social interaction with stranger 1 less than WT mice (**Fig. 12a and Table 3**). In the social novelty portion of the test, WT mice exhibited normal social novelty preference and interacted with stranger 2 for longer than they did with stranger 1 (**Fig. 12b and Table 3**). Additionally, we found no significant difference in reciprocal sniffing time between stranger 1 and stranger 2 in δ-catenin KO male and female mice (**Fig. 12b and Table 3**). Male and female δ-catenin KO mice engaged in social interaction with stranger 2 significantly less than the WT mice. (**Fig. 12b and Table 3**). These findings show that δ-catenin KO mice exhibit abnormal sociability and social novelty preference in the three-chamber test, like their G34S δ-catenin counterparts.

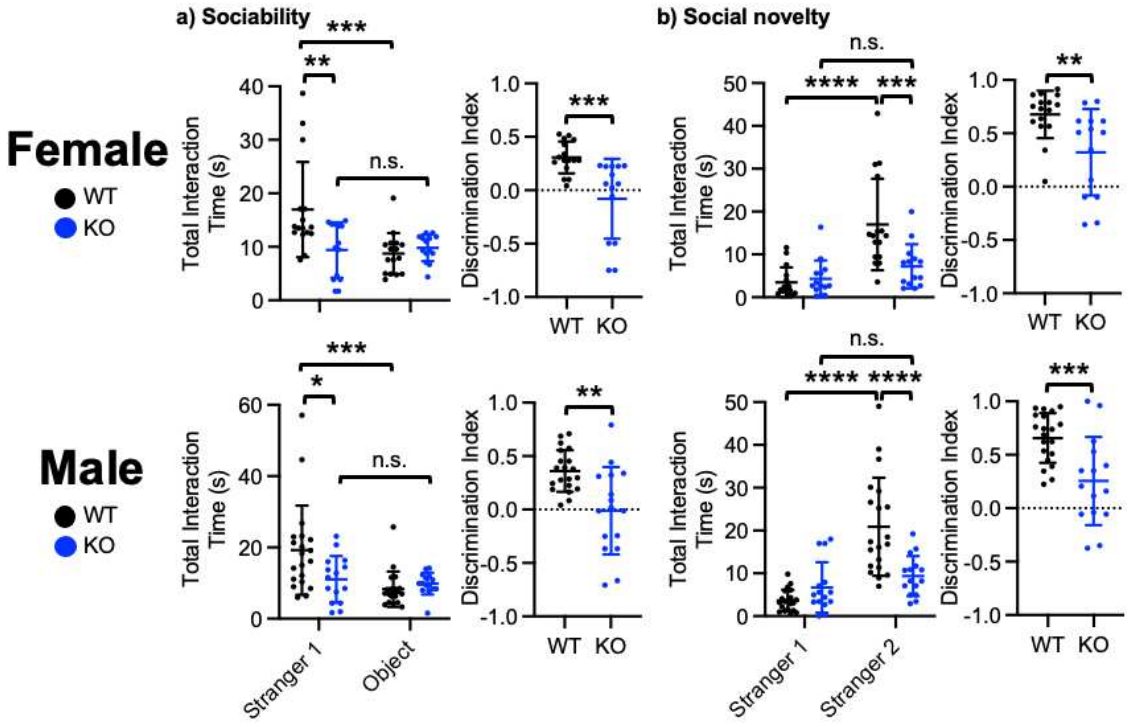

Figure 12. δ-catenin KO induces social dysfunction in mice.
Total interaction time and the discrimination index of **a)** sociability and **b)** social novelty in female and male WT and KO mice in the three-chamber test (n = number of animals, WT female = 16, KO female = 14, WT male = 20, and KO male = 15, **p* < 0.05, ***p* < 0.01, ****p* < 0.001, and *****p* < 0.0001, For total interaction time, Two-way ANOVA with Tukey test was used. For the discrimination index, the unpaired two-tailed Student's t-test was used. n.s. indicates no significant difference). Work done in part by Regan Roach.

Table 3. Three-chamber test summary of WT and KO mice.

Regular chow									
Female	WT (n = 16 mice)		KO (n = 14 mice)		Male	WT (n = 20 mice)		KO (n = 15 mice)	
Sociability	Stranger 1	Objective	Stranger 1	Objective	Sociability	Stranger 1	Objective	Stranger 1	Objective
Total Interaction Time (sec)	16.981 ± 8.908	8.731 ± 3.853	9.393 ± 5.173	9.829 ± 2.496	Total Interaction Time (sec)	19.225 ± 12.543	8.290 ± 4.968	11.053 ± 6.531	9.840 ± 3.052
	Stranger 1 vs. Objective, p = 0.0008		Stranger 1 vs. Objective, p = 0.9971			Stranger 1 vs. Objective, p = 0.0003		Stranger 1 vs. Objective, p = 0.9753	
	WT Stranger 1 vs. KO Stranger 1, p = 0.0035					WT Stranger 1 vs. KO Stranger 1, p = 0.0192			
Social novelty	Stranger 1	Stranger 2	Stranger 1	Stranger 2	Social novelty	Stranger 1	Stranger 2	Stranger 1	Stranger 2
Total Interaction Time (sec)	3.488 ± 3.466	16.994 ± 10.683	4.293 ± 4.296	7.221 ± 5.148	Total Interaction Time (sec)	3.670 ± 2.497	20.880 ± 11.455	6.713 ± 5.899	9.380 ± 4.679

	Stranger 1 vs. 2, $p < 0.0001$	Stranger 1 vs. 2, $p = 0.6511$		Stranger 1 vs. 2, $p < 0.0001$	Stranger 1 vs. 2, $p = 0.7403$
	WT Stranger 2 vs. KO Stranger 2, $p = 0.0010$			WT Stranger 2 vs. KO Stranger 2, $p < 0.0001$	

δ-catenin is required for lithium-induced restoration of normal social behavior in G34S mice.

Finally, to address whether δ-catenin is required for the positive effects of lithium on social behavior we used δ-catenin KO mice, which entirely lack δ-catenin expression. These δ-catenin KO mice were fed with the same lithium chow for 7 days prior to administration of the three-chamber test, and we then compared their social behavior to that of the lithium-treated δ-catenin G34S mice. When assessed the sociability we found no significant difference in total interaction time between stranger 1 and the novel object in lithium-treated male and female δ-catenin KO mice, an indicating abnormal sociability preference, unlike the normal sociability observed in G34S δ-catenin mice following lithium treatment (**Fig. 13a and Table 4**). Significantly, we found that social interaction with Stranger 1 in δ-catenin KO male and female mice was lower than G34S δ-catenin mice following lithium treatment (**Fig. 13a and Table 4.)** Following lithium treatment there was no significant difference in reciprocal sniffing time between stranger 1 and stranger 2 in δ-catenin KO male and female mice, indicating an abnormality in social novelty preference, unlike G34S mutant animals which exhibited normal social novelty preference following lithium treatment (**Fig. 13b and Table 4**). These findings demonstrate that δ-catenin is required for the restoration of normal social behavior in δ-catenin G34S mice following inhibition of GSK3β activity via lithium treatment.

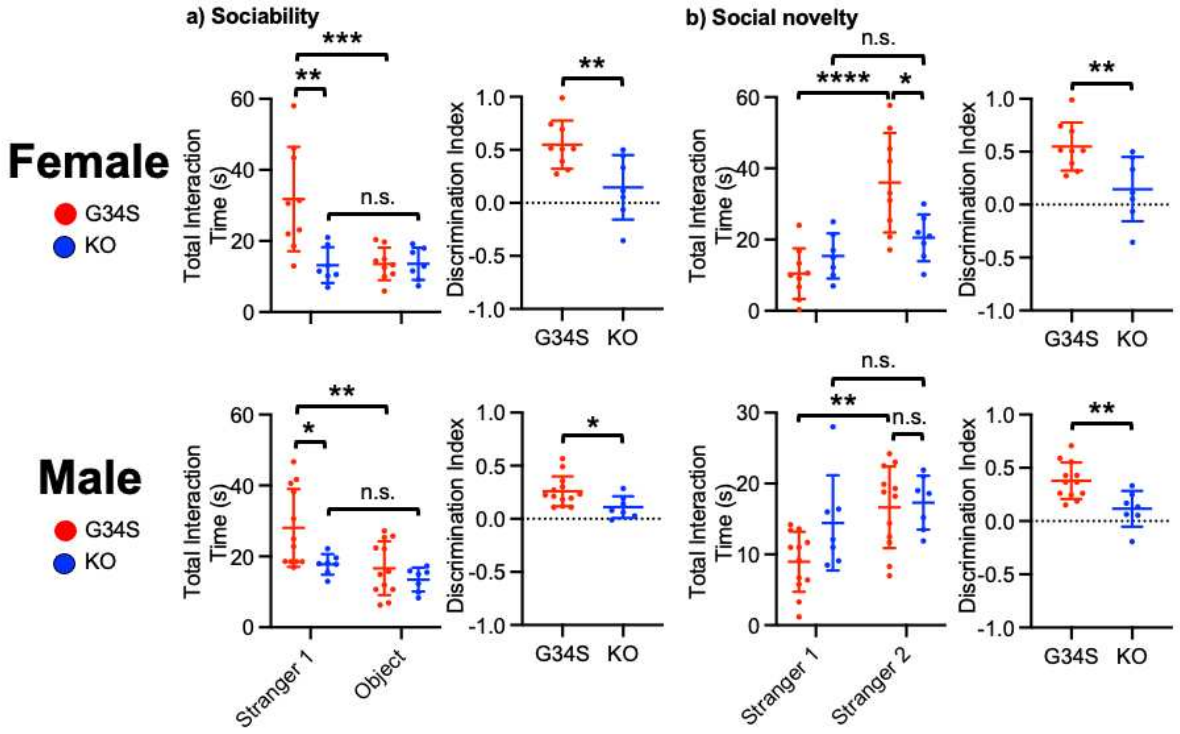

Figure 13. δ-catenin is required for lithium-induced restoration of normal social behavior in G34S mice.
Total interaction time and the discrimination index of **a)** sociability and **b)** social novelty in lithium-treated female and male G34S and KO mice in the three-chamber test (n = number of animals, G34S female + lithium = 9, KO female + lithium = 7, G34S male + lithium = 12, and KO male + lithium = 7, *$p < 0.05$, **$p < 0.01$, ***$p < 0.001$, and ****$p < 0.0001$, For total interaction time, Two-way ANOVA with Tukey test was used. For the discrimination index, the unpaired two-tailed Student's t-test was used. n.s. indicates no significant difference)

Table 4. Three-chamber test summary of G34S and KO mice with lithium chow.

Lithium chow									
Female	G34S (n = 9 mice)		KO (n = 7 mice)		Male	G34S (n = 12 mice)		KO (n = 7 mice)	
Sociability	Stranger 1	Objective	Stranger 1	Objective	Sociability	Stranger 1	Objective	Stranger 1	Objective
Total Interaction Time (sec)	31.800 ± 14.691	31.800 ± 14.691	13.200 ± 5.026	13.571 ± 4.549	Total Interaction Time (sec)	28.042 ± 10.979	16.667 ± 7.563	17.771 ± 2.906	13.457 ± 3.363
	Stranger 1 vs. Objective, $p = 0.0008$		Stranger 1 vs. Objective, $p = 0.9998$			Stranger 1 vs. Objective, $p = 0.0058$		Stranger 1 vs. Objective, $p = 0.7312$	
	WT Stranger 1 vs. G34S Stranger 1, $p = 0.0014$					WT Stranger 1 vs. G34S Stranger 1, $p = 0.0431$			

Social novelty	Stranger 1	Stranger 2	Stranger 1	Stranger 2	Social novelty	Stranger 1	Stranger 2	Stranger 1	Stranger 2
Total Interaction Time (sec)	10.433 ± 7.117	35.989 ± 13.988	15.371 ± 6.336	20.500 ± 6.562	Total Interaction Time (sec)	8.958 ± 4.248	16.650 ± 5.767	14.443 ± 6.724	17.300 ± 3.818
	Stranger 1 vs. 2, $p < 0.0001$		Stranger 1 vs. 2, $p = 0.7383$			Stranger 1 vs. 2, $p = 0.0011$		Stranger 1 vs. 2, $p = 0.7310$	
	WT Stranger 2 vs. G34S Stranger 2, $p = 0.0142$					WT Stranger 2 vs. G34S Stranger 2, $p > 0.9999$			

DISCUSSION

Autism spectrum disorder (ASD) is a multifactorial neurodevelopmental disorder that is commonly characterized by symptoms of impaired social communication, difficulty with social interaction, and restricted and repetitive behaviors (66). The pathophysiology of ASD is known to be largely influenced by strong genetic components throughout the early stages of development (66). The Simmons Foundation Autism Research Initiative (SFARI) gene database (https://gene.sfari.org) has documented over 1,000 candidate genes and copy number variations (CNVs) loci associated with ASD. Of these known ASD candidate genes, many are involved in synaptic formation, structure, and function (67). In fact, several molecular, cellular and functional studies of ASD in experimental models suggest that ASD pathogenesis is profoundly influenced by synaptic abnormalities (known as synaptopathy) (68). However, the mechanisms by which these gene products induce synaptopathy and ASD symptoms are not completely understood.

In recent years, the *δ-catenin* gene has been identified in multiple human genetic studies as strongly associated with ASD (12-16). Notably, the ASD-associated G34S mutation in the *δ-catenin* gene was found to cause a loss of δ-catenin function, irreversible by δ-catenin overexpression (16). Until now, the mechanisms underlying the ASD-associated δ-catenin missense mutation and the resulting loss of δ-catenin function have been relatively unknown, especially regarding how this loss of function contributes to ASD synaptopathy. Because the function of δ-catenin is highly correlated with other autism-risk genes that are involved in synaptic structure and function (23-26), our findings can potentially improve our understanding of the other mechanisms underlying ASD synaptopathy. In this study, we discovered that the G34S δ-catenin mutation can act as an additional site for phosphorylation by GSK3β. This increased phosphorylation results in the upregulated degradation of δ-catenin, an effect which we found can be adequately reversed by the inhibition of GSK3β activity. This key finding

enabled us to delve deeper into the role of δ-catenin function at the synapse, especially in GluA2 scaffolding, and allowed for a more profound investigation into how altered glutamatergic activity might induce the social dysfunction component of ASD.

We elected to use both the δ-catenin G34S knockin and our δ-catenin KO mouse model, to better clarify the role of δ-catenin in the glutamatergic activity of excitatory synapses and how δ-catenin deficiency results in disrupted social behavior. As both animal models exhibit similar profound social deficits, we demonstrate that the loss of function caused by the G34S δ-catenin mutation is functionally equivalent to the total absence of δ-catenin in the KO mouse model. Other data demonstrates that δ-catenin KO male and female mice show similar deficits in synaptic GluA2 as seen in G34S δ-catenin mice (**Fig. 7),** as well as similarly altered glutamatergic activity in cortical excitatory and inhibitory cells (36). Behaviorally, both the G34S δ-catenin mutant mice and the δ-catenin KO mice show the same social dysfunction. We found that inhibition of GSK3β activity is sufficient to reverse G34S δ-catenin-induced abnormal glutamatergic activity in excitatory and inhibitory cells and recover normal social behavior. To clarify that δ-catenin is necessary for the lithium-induced restoration of normal social behavior in δ-catenin G34S mice, our additional findings show that δ-catenin KO mice receive no behavioral benefit from the administration of lithium and instead remain socially impaired. This significantly strengthens our findings regarding the mechanism of lithium in the recovery of G34S δ-catenin function. Therefore, employment of both the δ-catenin G34S knockin and δ-catenin KO mouse lines allowed us to examine the δ-catenin-mediated neural mechanisms underlying social behavior more carefully.

In addition to the similarities in social behavior deficits, we further clarified that the loss of δ-catenin function via G34S mutation and genetic KO have similar opposing effects on glutamatergic activity in cortical excitatory and inhibitory cells (**Fig. 7c, 7d)** (36). However, the mechanism by which the loss of δ-catenin functions differentially affects cellular excitation and inhibition is unclear. Interestingly, GluA2-lacking AMPARs are Ca^{2+} permeable and have

increased single channel conductance, whereas GluA2-containing AMPA receptors are Ca^{2+} impermeable (69). Although cortical excitatory neurons possess no basal Ca^{2+}-permeable AMPAR (CP-AMPAR) expression, cortical inhibitory interneurons generally contain GluA2-lacking CP-AMPARs (70). It is possible that δ-catenin G34S and KO-induced reduction of GluA2 in excitatory cells may promote the expression or synaptic localization of highly conductive CP-AMPARs, thereby contributing to higher glutamatergic and neuronal activity.

Alternately, GluA1/2 or GluA2/3 heteromeric AMPA receptors are likely decreased in δ-catenin G34S and KO inhibitory interneurons, possibly leading to an overall decrease in glutamatergic and neuronal activity. In another experiment, we found that increased glutamatergic activity measured by Ca^{2+} imaging with glutamate uncaging in G34S δ-catenin excitatory cells is significantly decreased when treated with the CP-AMPAR blocker, NASPM (36). Our findings demonstrate that while δ-catenin deficiency generally lowers synaptic GluA2 levels in cortical neurons, it has opposing effects on glutamatergic and neuronal activity in excitatory and inhibitory cells. We believe this could be mediated by the recruitment of CP-AMPARs to the excitatory synapse, which warrants further investigation.

An additional explanation for our findings is that the loss of synaptic GluA2 merely results in reduced excitability in δ-catenin-deficient inhibitory neurons, thereby causing decreased activity of inhibitory neurons in their local circuits. This could result in a decrease in the action of inhibitory interneurons onto glutamatergic neurons, and thus allow for an increase of neuronal activity in these excitatory cells (disinhibition). A recent study has found that the loss of δ-catenin function by shRNA-mediated δ-catenin knockdown causes a significant decrease in the inhibition of cortical neurons resulting in increased excitation (26). Thus, δ-catenin loss may cause E/I imbalance due to decreased inhibitory interneuron function, thereby allowing the activity excitatory cells to go unchecked.

More specifically, research has suggested that parvalbumin-positive (PV+) inhibitory interneurons in the medial prefrontal cortex (mPFC) receive direct glutamatergic inputs from the

ventral hippocampus, basolateral amygdala, and mediodorsal thalamus (75-80). These inputs are thought to drive feedforward inhibition onto prefrontal pyramidal neurons, which may play a role in the regulation of social behavior (71-76). Thus, δ-catenin could be important for mediating the glutamatergic activity that excites PV+ inhibitory interneurons which then provide feedforward inhibition onto pyramidal neurons in the mPFC and regulate social behavior. δ-catenin deficiency-induced disinhibition could contribute to the increased neuronal activity in excitatory cells, particularly in the intact circuits, to cause social dysfunction. Finally, another recent study discovered that δ-catenin also localizes to inhibitory synapses (26). Therefore, it is possible that δ-catenin loss directly affects inhibitory GABAergic synapses to alter the E/I ratio. The multitude of possible explanations for our findings demonstrate that there are still many important questions to be answered to truly clarify the molecular mechanisms underlying the effect of δ-catenin deficiency on E/I balance.

Despite the increasing body of research investigating the molecular and cellular mechanisms of ASD, there is still strong lack of effective pharmacological approaches for treatment of ASD. This could be due in large part to broad variations in the origin and presentation of ASD in patients (77). Existing therapies are limited to the treatment of specific symptoms as opposed to addressing the basic underlying etiologies (78). This approach significantly limits the practicality of pharmaceutical intervention, especially for young ASD patients, as the benefit of treating individual symptoms may not outweigh the risk of adverse reactions and side effects. Thus, there is a strong need for increased research focusing on therapeutic agents that can more precisely target the underlying pathology of ASD. A myriad of studies have found GSK3β activity to be strongly implicated in the pathophysiology of ASD (27-34). Still, extensive studies have yet to yield consistent data explaining the role of GSK3β activity in the molecular and behavioral abnormalities associated with ASD.

Our study has identified GSK3β as a key target for the synaptic δ-catenin regulatory pathway and recognizes that GSK3β may perform well as new therapeutic target for limiting the

δ-catenin deficiency-induced synaptopathy in ASD. Moreover, we used the lithium treatment protocol to demonstrate that inhibition of GSK3β activity can sufficiently act as a therapeutic measure. Interestingly, there is strong evidence to suggest that lithium can act as a mood stabilizer by inhibiting GSK3β (79, 80). A significant therapeutic action of lithium is to regulate protein stability, particularly in synaptic proteins (35, 81). Interestingly, we previously reported that lithium reduces GSK3β activity and stabilizes synaptic δ-catenin, thus increasing the δ-catenin-GRIP/ABP-AMPAR complex at hippocampal synapses, and stabilizing synaptic activity (21). Our findings demonstrate that lithium is adequate for increasing synaptic δ-catenin and GluA2 levels in the cortex to enhance social behavior in mice. Significantly, lithium pharmacological intervention in 30 children and adolescents diagnosed with ASD was shown to improve symptoms in 43% of patients (82). Therefore, increasing δ-catenin levels at the synapse via the inhibition of GSK3β activity could stabilize synaptic AMPARs and spine integrity, which may be beneficial for ASD. Therefore, our work has enabled us to test a clinically relevant therapeutic treatment for ASD.

Other interesting findings in this study reveal possible sex-differences in δ-catenin expression. We found that total δ-catenin levels were significantly lower in the male G34S cortex compared to the male WT cortex. Moreover, total δ-catenin levels in the male G34S cortex were found to be distinctly lower than total δ-catenin levels in the female G34S cortex, where there was no difference in total δ-catenin levels between the WT and G34S animals (**Fig. 6**). Moreover, δ-catenin was found to be much higher in the male G34S cortex following lithium (**Fig. 7b**) as compared to female G34S cortex where lithium treatment was found to restore normal synaptic δ-catenin levels (**Fig. 7a**). This suggests that there are sex-differences in the regulation of δ-catenin levels. Analyzing potential sex-differences in neuropsychiatric research is critically important, especially due to the fact the males are diagnosed with ASD four times more often than females (83). The increased rate of ASD diagnoses in males is highly a complex issue, and could be due to a myriad of factors including genetic and hormonal differences as

well limitations in diagnostic criteria (84). Interestingly, the *δ-catenin* gene is known to be controlled by the estrogen signaling (85). Thus, possible that variations in δ-catenin regulation are based on the sex of animals, which presents an important direction for future research as sex differences in social behavioral abnormalities are common and not well understood (86).

Although this study establishes a mechanism for G34S δ-catenin loss of function and provides a drug target which we show is sufficient for reversal of social dysfunction in G34S δ-catenin mutant mice, there are a few key directions for future investigation which could address some of the limitations of this work. Most significantly, lithium is well established as a pharmaceutical inhibitor of GSK3β activity; however, lithium is also known to effect the activity of adenylyl cyclase, phosphoinositides and Protein kinase C (PKC), as well as alter the release of monoamine neurotransmitters, and arachidonic acid metabolism (21, 87). Because lithium may have several off-target effects, future aspects of this study could include other inhibitors of GSK3β to further clarify that inhibition of GSK3β contributes to the recovery of G34S δ-catenin function and social behavior in G34S δ-catenin mutant mice. Additionally, while we were able to demonstrate that decreasing GSK3β activity, both by lithium inhibition and by GSK3β siRNA knockdown, results in increased G34S δ-catenin (**Fig. 3a, 3b)**, we were unable to demonstrate that this cause-and-effect is due to physical interaction between GSK3β and G34S δ-catenin. Future aspects of this study could probe off target effects of lithium, and further clarify how GSK3β interacts with G34S δ-catenin.

REFERENCES

1. J. Ko, Neuroanatomical Substrates of Rodent Social Behavior: The Medial Prefrontal Cortex and Its Projection Patterns. *Front Neural Circuits* **11**, 41 (2017).
2. I. Rapin, R. Katzman, Neurobiology of autism. *Ann Neurol* **43**, 7-14 (1998).
3. W. C. Huang, Y. Chen, D. T. Page, Hyperconnectivity of prefrontal cortex to amygdala projections in a mouse model of macrocephaly/autism syndrome. *Nat Commun* **7**, 13421 (2016).
4. A. Selimbeyoglu *et al.*, Modulation of prefrontal cortex excitation/inhibition balance rescues social behavior in CNTNAP2-deficient mice. *Sci Transl Med* **9** (2017).
5. O. Yizhar *et al.*, Neocortical excitation/inhibition balance in information processing and social dysfunction. *Nature* **477**, 171-178 (2011).
6. W. Cao *et al.*, Gamma Oscillation Dysfunction in mPFC Leads to Social Deficits in Neuroligin 3 R451C Knockin Mice. *Neuron* **97**, 1253-1260 e1257 (2018).
7. F. Abell *et al.*, The neuroanatomy of autism: a voxel-based whole brain analysis of structural scans. *Neuroreport* **10**, 1647-1651 (1999).
8. F. Castelli, C. Frith, F. Happe, U. Frith, Autism, Asperger syndrome and brain mechanisms for the attribution of mental states to animated shapes. *Brain : a journal of neurology* **125**, 1839-1849 (2002).
9. N. Schmitz *et al.*, Neural correlates of executive function in autistic spectrum disorders. *Biological psychiatry* **59**, 7-16 (2006).
10. A. C. Brumback *et al.*, Identifying specific prefrontal neurons that contribute to autism-associated abnormalities in physiology and social behavior. *Molecular psychiatry* **23**, 2078-2089 (2018).
11. L. Liu *et al.*, Cell type-differential modulation of prefrontal cortical GABAergic interneurons on low gamma rhythm and social interaction. *Sci Adv* **6**, eaay4073 (2020).
12. I. O. Tuncay *et al.*, Analysis of recent shared ancestry in a familial cohort identifies coding and noncoding autism spectrum disorder variants. *NPJ Genom Med* **7**, 13 (2022).
13. D. E. Miller, A. Squire, J. T. Bennett, A child with autism, behavioral issues, and dysmorphic features found to have a tandem duplication within CTNND2 by mate-pair sequencing. *Am J Med Genet A* (2019).
14. H. Guo *et al.*, Inherited and multiple de novo mutations in autism/developmental delay risk genes suggest a multifactorial model. *Mol Autism* **9**, 64 (2018).
15. T. Wang *et al.*, De novo genic mutations among a Chinese autism spectrum disorder cohort. *Nat Commun* **7**, 13316 (2016).
16. T. N. Turner *et al.*, Loss of delta-catenin function in severe autism. *Nature* **520**, 51-56 (2015).
17. K. S. Kosik, C. P. Donahue, I. Israely, X. Liu, T. Ochiishi, Delta-catenin at the synaptic-adherens junction. *Trends Cell Biol* **15**, 172-178 (2005).

18. J. B. Silverman *et al.*, Synaptic anchorage of AMPA receptors by cadherins through neural plakophilin-related arm protein AMPA receptor-binding protein complexes. *J Neurosci* **27**, 8505-8516 (2007).
19. L. Yuan, E. Seong, J. L. Beuscher, J. Arikkath, delta-Catenin Regulates Spine Architecture via Cadherin and PDZ-dependent Interactions. *The Journal of biological chemistry* **290**, 10947-10957 (2015).
20. J. Gilbert, H. Y. Man, The X-Linked Autism Protein KIAA2022/KIDLIA Regulates Neurite Outgrowth via N-Cadherin and delta-Catenin Signaling. *eNeuro* **3** (2016).
21. M. Farooq *et al.*, Lithium increases synaptic GluA2 in hippocampal neurons by elevating the delta-catenin protein. *Neuropharmacology* (2016).
22. S. Restituito *et al.*, Synaptic autoregulation by metalloproteases and gamma-secretase. *J Neurosci* **31**, 12083-12093 (2011).
23. S. Ramanathan *et al.*, A case of autism with an interstitial deletion on 4q leading to hemizygosity for genes encoding for glutamine and glycine neurotransmitter receptor sub-units (AMPA 2, GLRA3, GLRB) and neuropeptide receptors NPY1R, NPY5R. *BMC Med Genet* **5**, 10 (2004).
24. A. El-Amraoui, C. Petit, Cadherins as targets for genetic diseases. *Cold Spring Harb Perspect Biol* **2**, a003095 (2010).
25. R. Mejias *et al.*, Gain-of-function glutamate receptor interacting protein 1 variants alter GluA2 recycling and surface distribution in patients with autism. *Proc Natl Acad Sci U S A* **108**, 4920-4925 (2011).
26. N. Assendorp *et al.*, CTNND2 moderates neuronal excitation and links human evolution to prolonged synaptic development in the neocortex. *bioRxiv*, 2022.2009.2013.507776 (2022).
27. W. W. Min *et al.*, Elevated glycogen synthase kinase-3 activity in Fragile X mice: key metabolic regulator with evidence for treatment potential. *Neuropharmacology* **56**, 463-472 (2009).
28. C. J. Yuskaitis *et al.*, Lithium ameliorates altered glycogen synthase kinase-3 and behavior in a mouse model of fragile X syndrome. *Biochemical pharmacology* **79**, 632-646 (2010).
29. E. J. McManus *et al.*, Role that phosphorylation of GSK3 plays in insulin and Wnt signalling defined by knockin analysis. *Embo J* **24**, 1571-1583 (2005).
30. M. A. Mines, C. J. Yuskaitis, M. K. King, E. Beurel, R. S. Jope, GSK3 influences social preference and anxiety-related behaviors during social interaction in a mouse model of fragile X syndrome and autism. *PLoS One* **5**, e9706 (2010).
31. C. H. Kwon *et al.*, Pten regulates neuronal arborization and social interaction in mice. *Neuron* **50**, 377-388 (2006).
32. Y. Mao *et al.*, Disrupted in schizophrenia 1 regulates neuronal progenitor proliferation via modulation of GSK3beta/beta-catenin signaling. *Cell* **136**, 1017-1031 (2009).
33. W. Y. Kim, W. D. Snider, Functions of GSK-3 Signaling in Development of the Nervous System. *Frontiers in molecular neuroscience* **4**, 44 (2011).
34. X. Wu *et al.*, Lithium ameliorates autistic-like behaviors induced by neonatal isolation in rats. *Front Behav Neurosci* **8**, 234 (2014).
35. O. O'Leary, Y. Nolan, Glycogen synthase kinase-3 as a therapeutic target for cognitive dysfunction in neuropsychiatric disorders. *CNS Drugs* **29**, 1-15 (2015).

36. H. Mendez-Vazquez *et al.*, The autism-associated loss of δ-catenin functions disrupts social behaviors. *bioRxiv*, 2023.2001.2012.523372 (2023).
37. S. Kim, E. B. Ziff, Calcineurin mediates synaptic scaling via synaptic trafficking of Ca2+-permeable AMPA receptors. *PLoS biology* **12**, e1001900 (2014).
38. K. Sztukowski *et al.*, HIV induces synaptic hyperexcitation via cGMP-dependent protein kinase II activation in the FIV infection model. *PLoS biology* **16**, e2005315 (2018).
39. S. Kim, A. N. Lapham, C. G. Freedman, T. L. Reed, W. K. Schmidt, Yeast as a tractable genetic system for functional studies of the insulin-degrading enzyme. *The Journal of biological chemistry* **280**, 27481-27490 (2005).
40. S. Kim *et al.*, Brain region-specific effects of cGMP-dependent kinase II knockout on AMPA receptor trafficking and animal behavior. *Learning & memory* **23**, 435-441 (2016).
41. S. Kim *et al.*, Evidence that the rab5 effector APPL1 mediates APP-betaCTF-induced dysfunction of endosomes in Down syndrome and Alzheimer's disease. *Molecular psychiatry* (2015).
42. S. Kim, J. Shou, S. Abera, E. B. Ziff, Sucrose withdrawal induces depression and anxiety-like behavior by Kir2.1 upregulation in the nucleus accumbens. *Neuropharmacology* **130**, 10-17 (2018).
43. S. Kim *et al.*, Network compensation of cyclic GMP-dependent protein kinase II knockout in the hippocampus by Ca2+-permeable AMPA receptors. *Proc Natl Acad Sci U S A* **112**, 3122-3127 (2015).
44. S. Kim, C. J. Violette, E. B. Ziff, Reduction of increased calcineurin activity rescues impaired homeostatic synaptic plasticity in presenilin 1 M146V mutant. *Neurobiol Aging* **36**, 3239-3246 (2015).
45. J. P. Roberts, S. A. Stokoe, M. F. Sathler, R. A. Nichols, S. Kim, Selective co-activation of alpha7- and alpha4beta2-nicotinic acetylcholine receptors reverses beta-amyloid-induced synaptic dysfunction. *The Journal of biological chemistry*, 100402 (2021).
46. M. F. Sathler *et al.*, HIV and FIV glycoproteins increase cellular tau pathology via cGMP-dependent kinase II activation. *Journal of cell science* **135** (2022).
47. M. F. Sathler *et al.*, Phosphorylation of the AMPA receptor subunit GluA1 regulates clathrin-mediated receptor internalization. *Journal of cell science* **134** (2021).
48. J. Shou, A. Tran, N. Snyder, E. Bleem, S. Kim, Distinct Roles of GluA2-lacking AMPA Receptor Expression in Dopamine D1 or D2 Receptor Neurons in Animal Behavior. *Neuroscience* **398**, 102-112 (2018).
49. J. L. Sun *et al.*, Co-activation of selective nicotinic acetylcholine receptors is required to reverse beta amyloid-induced Ca(2+) hyperexcitation. *Neurobiol Aging* **84**, 166-177 (2019).
50. T. M. Tran *et al.*, Loss of cGMP-dependent protein kinase II alters ultrasonic vocalizations in mice, a model for speech impairment in human microdeletion 4q21 syndrome. *Neuroscience letters* **759**, 136048 (2021).
51. A. Zaytseva *et al.*, Ketamine’s rapid antidepressant effects are mediated by Ca²⁺-permeable AMPA receptors in the hippocampus. *bioRxiv*, 2022.2012.2005.519102 (2023).

52. A. Zaytseva *et al.*, Ketamine's rapid antidepressant effects are mediated by Ca²⁺-permeable AMPA receptors in the hippocampus. *bioRxiv*, 2022.2012.2005.519102 (2022).
53. J. Y. Kim *et al.*, Viral transduction of the neonatal brain delivers controllable genetic mosaicism for visualising and manipulating neuronal circuits in vivo. *The European journal of neuroscience* **37**, 1203-1220 (2013).
54. H. Dana *et al.*, High-performance calcium sensors for imaging activity in neuronal populations and microcompartments. *Nature methods* **16**, 649-657 (2019).
55. J. Dimidschstein *et al.*, A viral strategy for targeting and manipulating interneurons across vertebrate species. *Nat Neurosci* **19**, 1743-1749 (2016).
56. S. Kim *et al.*, Neural circuit pathology driven by Shank3 mutation disrupts social behaviors. *Cell Rep* **39**, 110906 (2022).
57. S. Kim, Y. E. Kim, I. H. Kim, Simultaneous analysis of social behaviors and neural responses in mice using round social arena system. *STAR Protoc* **3**, 101722 (2022).
58. S. Bareiss, K. Kim, Q. Lu, Delta-catenin/NPRAP: A new member of the glycogen synthase kinase-3beta signaling complex that promotes beta-catenin turnover in neurons. *Journal of neuroscience research* **88**, 2350-2363 (2010).
59. M. Oh *et al.*, GSK-3 phosphorylates delta-catenin and negatively regulates its stability via ubiquitination/proteosome-mediated proteolysis. *The Journal of biological chemistry* **284**, 28579-28589 (2009).
60. D. W. Harms *et al.*, Mouse Genome Editing Using the CRISPR/Cas System. *Curr Protoc Hum Genet* **83**, 15 17 11-27 (2014).
61. J. L. Rubenstein, M. M. Merzenich, Model of autism: increased ratio of excitation/inhibition in key neural systems. *Genes Brain Behav* **2**, 255-267 (2003).
62. G. K. Beauchamp, K. Yamazaki, Chemical signalling in mice. *Biochemical Society transactions* **31**, 147-151 (2003).
63. M. Yang, J. N. Crawley, Simple behavioral assessment of mouse olfaction. *Current protocols in neuroscience / editorial board, Jacqueline N. Crawley ... [et al.]* **Chapter 8**, Unit 8 24 (2009).
64. A. K. Beery, D. Kaufer, Stress, social behavior, and resilience: insights from rodents. *Neurobiol Stress* **1**, 116-127 (2015).
65. M. Yang, J. L. Silverman, J. N. Crawley, Automated three-chambered social approach task for mice. *Current protocols in neuroscience / editorial board, Jacqueline N. Crawley ... [et al.]* **Chapter 8**, Unit 8 26 (2011).
66. S. Guang *et al.*, Synaptopathology Involved in Autism Spectrum Disorder. *Frontiers in cellular neuroscience* **12**, 470 (2018).
67. J. Gilbert, H. Y. Man, Fundamental Elements in Autism: From Neurogenesis and Neurite Growth to Synaptic Plasticity. *Frontiers in cellular neuroscience* **11**, 359 (2017).
68. H. Won, W. Mah, E. Kim, Autism spectrum disorder causes, mechanisms, and treatments: focus on neuronal synapses. *Frontiers in molecular neuroscience* **6**, 19 (2013).
69. G. H. Diering, R. L. Huganir, The AMPA Receptor Code of Synaptic Plasticity. *Neuron* **100**, 314-329 (2018).

70. J. T. Isaac, M. C. Ashby, C. J. McBain, The role of the GluR2 subunit in AMPA receptor function and synaptic plasticity. *Neuron* **54**, 859-871 (2007).
71. R. Marek *et al.*, Hippocampus-driven feed-forward inhibition of the prefrontal cortex mediates relapse of extinguished fear. *Nat Neurosci* **21**, 384-392 (2018).
72. Q. Sun *et al.*, Ventral Hippocampal-Prefrontal Interaction Affects Social Behavior via Parvalbumin Positive Neurons in the Medial Prefrontal Cortex. *iScience* **23**, 100894 (2020).
73. A. C. Felix-Ortiz, A. Burgos-Robles, N. D. Bhagat, C. A. Leppla, K. M. Tye, Bidirectional modulation of anxiety-related and social behaviors by amygdala projections to the medial prefrontal cortex. *Neuroscience* **321**, 197-209 (2016).
74. L. M. McGarry, A. G. Carter, Inhibitory Gating of Basolateral Amygdala Inputs to the Prefrontal Cortex. *J Neurosci* **36**, 9391-9406 (2016).
75. B. R. Ferguson, W. J. Gao, Thalamic Control of Cognition and Social Behavior Via Regulation of Gamma-Aminobutyric Acidergic Signaling and Excitation/Inhibition Balance in the Medial Prefrontal Cortex. *Biological psychiatry* **83**, 657-669 (2018).
76. K. Delevich, J. Tucciarone, Z. J. Huang, B. Li, The mediodorsal thalamus drives feedforward inhibition in the anterior cingulate cortex via parvalbumin interneurons. *J Neurosci* **35**, 5743-5753 (2015).
77. R. E. Accordino, C. Kidd, L. C. Politte, C. A. Henry, C. J. McDougle, Psychopharmacological interventions in autism spectrum disorder. *Expert Opin Pharmacother* **17**, 937-952 (2016).
78. D. R. Hampson, S. Gholizadeh, L. K. Pacey, Pathways to drug development for autism spectrum disorders. *Clin Pharmacol Ther* **91**, 189-200 (2012).
79. W. T. O'Brien, P. S. Klein, Validating GSK3 as an in vivo target of lithium action. *Biochemical Society transactions* **37**, 1133-1138 (2009).
80. D. M. Chuang, H. K. Manji, In search of the Holy Grail for the treatment of neurodegenerative disorders: has a simple cation been overlooked? *Biological psychiatry* **62**, 4-6 (2007).
81. C. Xu, N. G. Kim, B. M. Gumbiner, Regulation of protein stability by GSK3 mediated phosphorylation. *Cell cycle* **8**, 4032-4039 (2009).
82. M. Siegel *et al.*, Preliminary investigation of lithium for mood disorder symptoms in children and adolescents with autism spectrum disorder. *J Child Adolesc Psychopharmacol* **24**, 399-402 (2014).
83. T. May, I. Adesina, J. McGillivray, N. J. Rinehart, Sex differences in neurodevelopmental disorders. *Curr Opin Neurol* **32**, 622-626 (2019).
84. K. Dworzynski, A. Ronald, P. Bolton, F. Happé, How different are girls and boys above and below the diagnostic threshold for autism spectrum disorders? *J Am Acad Child Adolesc Psychiatry* **51**, 788-797 (2012).
85. G. V. Raj *et al.*, Estrogen receptor coregulator binding modulators (ERXs) effectively target estrogen receptor positive human breast cancers. *Elife* **6** (2017).
86. E. Choleris, L. A. M. Galea, F. Sohrabji, K. M. Frick, Sex differences in the brain: Implications for behavioral and biomedical research. *Neuroscience and biobehavioral reviews* **85**, 126-145 (2018).

87. F. Marmol, Lithium: bipolar disorder and neurodegenerative diseases Possible cellular mechanisms of the therapeutic effects of lithium. *Prog Neuropsychopharmacol Biol Psychiatry* **32**, 1761-1771 (2008).